

Dissertationes Forestales 298

Effects of long-term moisture and weather exposure on
the structure and properties of thermally modified wood

Chenyang Cai

School of Forest Sciences,
Faculty of Science and Forestry,
University of Eastern Finland

Academic Dissertation

To be presented by permission of the Faculty of Science and Forestry for online public examination at the University of Eastern Finland, Joensuu, on June 12, 2020, at 12 o'clock

Title of dissertation: Effects of long-term moisture and weather exposure on the structure and properties of thermally modified wood

Author: Chenyang Cai

Dissertationes Forestales 298

<https://doi.org/10.14214/df.298>

Use licence [CC BY-NC-ND 4.0](https://creativecommons.org/licenses/by-nc-nd/4.0/)

Thesis supervisors:

Dr. Henrik Heräjärvi

Natural Resources Institute Finland, Joensuu, Finland

Assoc. Professor Antti Haapala

School of Forest Sciences, University of Eastern Finland, Finland

Pre-examiners:

Professor Holger Militz

Depart. of Wood Biology and Wood Products, Georg-August-Universität, Germany

Professor Magnus Wålinder

Depart. of Civil and Architectural Engineering, KTH Royal Institute of Technology, Sweden

Opponent:

Assoc. Professor Emil Engelund Thybring

Depart. of Geosciences and Natural Resource Management, University of Copenhagen, Denmark

ISSN 1795-7389 (online)

ISBN 978-951-651-686-1 (pdf)

ISSN 2323-9220 (print)

ISBN 978-951-651-687-8 (paperback)

Publishers:

Finnish Society of Forest Science

Faculty of Agriculture and Forestry of the University of Helsinki

School of Forest Sciences of the University of Eastern Finland

Editorial office:

Finnish Society of Forest Science

Viikinkaari 6, Fi-00790 Helsinki, Finland

<http://www.dissertationesforestales.fi>

Cai C. (2020). Effects of long-term moisture and weather exposure on the structure and properties of thermally modified wood. *Dissertationes Forestales* 298. 50 p.
<https://doi.org/10.14214/df.298>

ABSTRACT

Thermal modification (TM) has been widely used to improve the dimensional stability and durability of wood. However, the performance of thermally modified wood (TMW) in conditions where it must endure continuous changes in ambient moisture content are not entirely clear. This thesis investigated the chemical components, cellular structure, and physical properties of thermally modified Scots pine, Norway spruce, and European ash wood exposed to long-term water contact condition, different temperature and relative humidity condition and natural weather condition.

The results showed that increase in TM intensity reduced the equilibrium moisture content (EMC) and improved the dimensional stability of wood mostly in a tangential direction. TM did not affect Brinell hardness, while increase in EMC decreased wood hardness. Prolonged exposure to water mainly changed hemicelluloses and cellulose and increases the hygroscopicity of both modified and unmodified wood. In addition, the initial higher acidity of TMW tends to promote the degradation of the cell-wall compounds, resulting in faster degradation in TMW than in unmodified wood during water contact exposure.

Degradation of lignin and leaching of the degradation products during the weathering exposure leaves wood with a grey hue and surface with higher relative cellulose and hemicellulose content. TMW presented less changes in lignin structure and color due to its condensed lignin structure and lower hygroscopicity compared to unmodified wood. The lower EMC and fiber saturation point (FSP) value of TMW compared to unmodified wood indicates that TM can limit water absorption during weathering. Therefore, TMW showed less cupping than unmodified wood in wet conditions. Brinell hardness was slightly decreased in all specimens due to cell wall degradation and increase in EMC. Additionally, increase in the TM intensity improved weathering performance of wood by reducing the surface chemical changes, water accessibility and cell wall porosity.

Keywords: chemistry, degradation, physical properties, microstructure, thermally modified wood, weathering

ACKNOWLEDGEMENTS

The studies described in this thesis were mainly performed at the School of Forest Sciences at the University of Eastern Finland. The studies were financially supported by the University of Eastern Finland, the International ThermoWood Association, Jenny and Antti Wihuri Foundation, Finnish Cultural Foundation and Teollisuusneuvos Heikki Väänänen's Fund.

I would like to express my sincere gratitude to the people who helped me to complete this thesis. I am grateful to my main supervisor, Dr. Henrik Heräjärvi, who introduced me to this field of research. His guidance, support and encouragement throughout the research process have been invaluable to me. I am also grateful to my supervisor, Dr. Antti Haapala, for his patient advice, mentoring, support and sharing his expertise.

I would like to thank my co-authors: Dr. Jukka Antikainen, Dr. Katri Luostarinen, Dr. Kirsi Mononen, Dr. Muhammad Asadullah Javed, Dr. Sanna Komulainen, Prof. Ville-Veikko Telkki, Mr. Mohammad Habibur Rahman, Dr. Markku Tiitta, Mr. Valtteri Tiitta, Dr. Laura Tomppo and Prof. Reijo Lappalainen, for their cooperation and contributions to improving this research. Mr. Risto Ikonen, Mr. Jarmo Pennala and Mr. Juhani Marttila are thanked for preparing wood specimens and experimental setup. Botanical garden Botania in Joensuu, Finland, is acknowledged for accommodating the weather exposure test setup between 2016 and 2018. Ms. Maini Mononen and Ms. Leena Kuusisto are thanked for helping with laboratory-related issues. I would also like to thank all my colleagues and friends in Finland for their help and moments we have shared together.

The pre-examiners of this thesis, Prof. Holger Militz and Prof. Magnus Wålinder, are thanked for their valuable comments and suggestions.

Finally, I would like to give my heartfelt thanks to my parents for their care and support throughout my life, and Mr. Xiao Zhou for his understanding and encouragement

Nanjing, 20th May 2020
Chenyang Cai

LIST OF ORIGINAL PUBLICATIONS

This thesis is based on data presented in the following articles, referred to by the Roman Numerals I–IV

- I. Cai C., Antikainen J., Luostarinen K., Mononen K., Heräjärvi H. (2018). Wetting-induced changes on the surface of thermally modified Scots pine and Norway spruce wood. *Wood Science and Technology* 52: 1181–1193.
doi: 10.1007/s00226-018-1030-1
- II. Cai C., Heräjärvi H., Haapala A. (2019). Effects of environmental conditions on physical and mechanical properties of thermally modified wood. *Canadian Journal of Forest Research* 49: 1434–1440.
doi: 10.1139/cjfr-2019-0180
- III. Cai C., Haapala A., Rahman MH., Tiitta M., Tiitta V., Tomppo L., Lappalainen R., Heräjärvi H. (2020) Effects of Two-year Weather Exposure on Thermally Modified *Picea abies*, *Pinus sylvestris*, and *Fraxinus excelsior* Wood. *Canadian Journal of Forest Research* (in press)
- IV. Cai C., Javed MA., Komulainen S., Telkki V-V., Haapala A., Heräjärvi H. (2020). Effect of natural weathering on water absorption and pore size distribution in thermally modified wood determined by nuclear magnetic resonance. *Cellulose* 27: 4235–4247
doi: 10.1007/s10570-020-03093-x

The present author was the principal author of all the papers, with the main responsibility for the experimental design and realization, analysis and reporting of the results. The results were also partly analyzed and reported by the second author in Paper I, the third, fourth, fifth and sixth author in Paper III and the second and third authors in Paper IV. The other co-authors participated in the experimental design and writing of the papers.

CONTENTS

1 INTRODUCTION	9
1.1 Background and motivation	9
1.2 Chemistry and structure of wood	9
1.2.1 Chemical composition of wood	9
1.2.2 Wood structure	12
1.2.3 Cell wall structure	12
1.3 Water in wood	13
1.4 Thermal modification process	15
1.5 Effects of exposure conditions on wood	17
1.5.1 Changes in wood due to thermal modification	17
1.5.2 Changes in wood due to moisture and liquid water	18
1.5.3 Changes in wood due to weathering	19
1.6 Gaps in knowledge	21
1.7 Research objectives	21
2 MATERIALS AND METHODS	21
2.1 Study materials and thermal modification	21
2.2 Long-term water contact exposure test	22
2.3 Controlled T-RH weather chamber test	22
2.4 Outdoor weather exposure test	22
2.5 Analyses of wood specimens	23
2.5.1 Overview of experimental material	23
2.5.2 Chemical properties	24
2.5.3 Anatomic structure	25
2.5.4 Physical properties	25
3 RESULTS AND DISCUSSION	29
3.1 Changes of wood due to moisture and liquid water exposure	29
3.1.1 Chemical composition and pH of wood (Paper I)	29
3.1.2 Microstructure (Paper I)	30
3.1.3 EMC, swelling, and shrinkage (Paper II)	31
3.1.4 Brinell hardness (Paper II)	32
3.2 Changes in wood due to natural weathering	33
3.2.1 Chemical composition and pH of wood (Paper III)	33
3.2.2 Pore size distribution in cell walls (Paper IV)	35
3.2.3 Wood-water interaction (Papers III and IV)	36
3.2.4 Wood appearance (Paper III)	38
3.2.5 Basic density and Brinell hardness (Paper III)	40
3.3 Reliability and validity of the results	41
4 CONCLUSIONS	42
5 REFERENCES	44

LIST OF ABBREVIATIONS

CPMG	Carr-Purcell-Meiboom-Gill
EMC	equilibrium moisture content
FSP	fiber saturation point
FTIR	Fourier transform infrared
LWC	long-term water contact
MC	moisture content
MRI	Magnetic resonance imaging
NMR	nuclear magnetic resonance
NW	natural weathering
RH	relative humidity
TM	thermal modification
TMW	thermally modified wood
T-RH	temperature - relative humidity
T ₂	spin-spin relaxation time

1 INTRODUCTION

1.1 Background and motivation

Wood has significant advantages such as ubiquitous resources, good mechanical performance combined with relative low density, and easy process ability. Rising consciousness of carbon emissions, sustainability and overall environmental impact has positioned wood as a powerful and valuable solution for a construction material. However, particularly in outdoor applications, the exposed wood loses its performance gradually due to many reasons, such as sunlight, wetting and drying through precipitation, diurnal and seasonal changes in relative humidity (RH), temperature changes, abrasion by windblown materials, pollutants, decomposition by microbes and various human activities (Williams 2005). Therefore, wood modification, application of chemical, physical, or biological methods to alter the properties and gain better wood performance, has become indispensable. Modification technologies include densification, resin impregnation, chemical modification of the cell wall components, and thermal modification (e.g., Hill 2006).

Thermal modification (TM) improves the dimensional stability and decay resistance of wood, enabling its use in outdoor applications, most typically in decking, window frames, cladding and garden furniture. The main species thermally modified are softwoods, such as Scots pine (*Pinus sylvestris*) and Norway spruce (*Picea abies*), but valuable hardwoods like ash (*Fraxinus excelsior*) and Fraké (*Terminalia superba*) are of growing interest in markets due to their higher strength and beautiful appearance.

In comparison to untreated wood, thermally modified wood (TMW) is reported to be less susceptible to water- and weather-induced degradation, due to its reduced hygroscopicity and crosslinked lignin structure (Nuopponen et al. 2004; Metsä-Kortelainen et al. 2006; Yildiz et al. 2011; Tomak et al. 2014). However, such a protective effect has been reported to cease/decrease gradually after long-term exposure (Huang et al. 2012; Srinivas and Pandey 2012; Xing et al. 2015).

To understand the behavior of TMW in a real end use environment, this thesis presents work carried out to characterize the properties of thermally modified Scots pine, Norway spruce, and European ash wood after being exposed to water, different temperatures and relative humidity, as well as natural weathering for extended periods of time. The results of this study help in understanding the performance of TMW in its end-use applications.

1.2 Chemistry and structure of wood

1.2.1 Chemical composition of wood

Wood is a natural polymeric material, which is mainly composed of cellulose, hemicelluloses, lignin and a minor portion of extractives (<5% of dry wood mass) (Fengel and Wegener 1989, Sjöström 1993). Cellulose, hemicellulose, and lignin are the structural components of the wood cell wall, whilst the extractives are non-structural and low-molecular-mass compounds present in smaller quantities and in greater variation between species, deposited primarily in heartwood (Figure 1, Fengel and Wegener 1989).

Cellulose

Cellulose that accounts for 40–50% of dry wood mass, is the main polymeric component of the wood cell wall, consisting of a linear chain of β -D-glucopyranoses in groups of two sugar units called cellobiose joined by 1 to 4 glycosidic bonds. Cellulose molecules aggregate into bundles called elementary fibrils through the intra- and intermolecular hydrogen bonds formed between the hydroxyl (-OH) groups in cellulose, and these elementary fibrils aggregate forming microfibrils surrounded by amorphous hemicelluloses and lignin (Figure 1, Fengel and Wegener 1989). Microfibrils are constituted of parallelly aligned crystalline regions and disordered amorphous regions stabilized by van der Waals interactions and hydrogen bonding. Bundles of microfibrils are further organized into larger elements called fibrils, which finally build up the wood fiber cell wall (Thomas 1977).

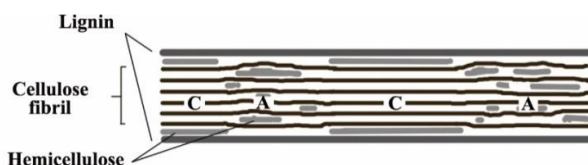


Figure 1. Longitudinal section of an elementary fibril model showing the crystalline (C) and amorphous (A) regions of cellulose, accompanied by hemicelluloses, both embedded in lignin matrix.

Hemicelluloses

Compared with cellulose, hemicelluloses are shorter, amorphous and branched carbohydrate molecules that consist of predominantly five sugar units: glucose, mannose, galactose, xylose and arabinose. The other constituents of the hemicelluloses are some moieties of hexuronic acids and deoxyhexoses (Fengel and Wegener 1989; Sjöström 1993). Hemicelluloses proportions are approximately 20–25% and 25–30% of the dry wood mass in softwoods and hardwoods, respectively, and the chemical composition of hemicelluloses also differ between softwoods and hardwoods. In softwoods, the most abundant hemicellulose is galactoglucomannans, whilst in hardwoods, the main hemicellulose is glucuronoxylans (Sjöström 1993).

The hemicelluloses play an important role in bonding microfibrils together and strengthening the woody skeleton. They might also be present within amorphous regions of cellulose microfibrils (Vincent 1999, Salmén 2004). Hemicelluloses are less stable than cellulose and lignin upon heating (Figure 2). The changes of chemical compositions due to TM are introduced in Chapter 1.5.1.

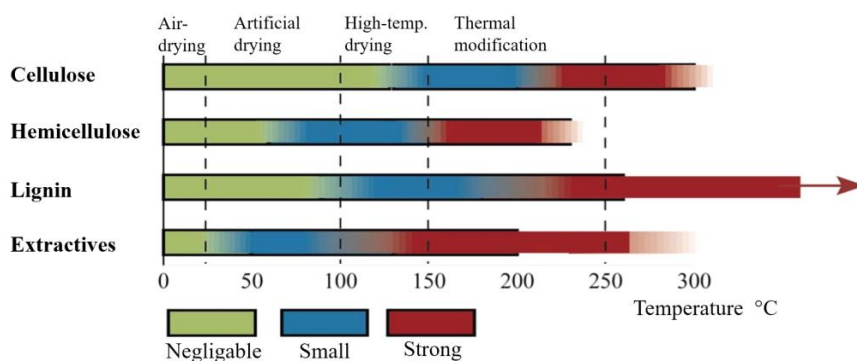


Figure 2. General changes of wood components under humid condition at different temperatures (reprinted [adapted] with permission from Sundqvist, 2004 © Luleå University of Technology).

Lignin

Lignin is a common name for complex, three-dimensionally branched, hydrophobic, amorphous polymers of a number of phenylpropane monomer units, occurring between the middle lamella surrounding individual wood cells and within the cell walls, considered as a natural adhesive. The share of lignin is approximately 25–30% and 20–25% of the dry wood mass in softwoods and hardwoods, respectively; and it is often considered to be the stiffening agent to reinforce wood structure (Fengel and Wegener 1989; Sjöström 1993; Glasser 2019). The principal chemical component of softwoods' lignin is guaiacyl (Figure 3, Laurichesse and Avérous 2014). The ratio of guaiacyl and the other main component, syringyl, in softwood is approximately 10:1. Lignin in hardwoods is referred to as guaiacyl-syringyl lignin, because the guaiacyl and syringyl unit ratios vary from 4:1 to 1:2 (Sjöström 1993). The guaiacyl unit has more reactive sites and crosslinking potential than the syringyl unit, making softwood lignin relatively more difficult to be degraded than hardwood lignin (Thomas 1977). The small variability of native lignin composition in wood, within species, seems to be limited to differences between middle lamella and cell wall lignin, to differences between juvenile and mature plant tissue, and to differences in function (bonding as opposed to stiffening needs) (Monties 2003).

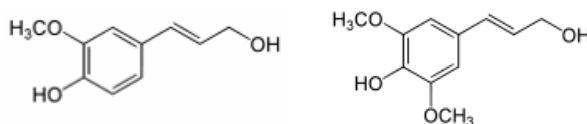


Figure 3. Guaiacyl lignin monomer unit (left), Syringyl lignin monomer unit (right).

Extractives

Extractives are non-structural, low-molecular-mass wood components which comprise a wide range of organic (terpenoids, steroids, fats, waxes, phenolic compounds) and inorganic

(calcium, potassium, magnesium, carbonates, silicates) compounds (Thomas 1977, Fengel and Wegener 1989, Sjöström 1993). They exist as monomers, dimers, and polymers and can be removed from wood by extraction with hot or cold water or organic solvents. Although extractives occur in wood in small quantities, they show essential contributions to wood materials, for example to color, odor, decay resistance, density, hygroscopicity, and flammability (Fengel and Wegener 1989). Some of the extractives in wood are precursors to other chemicals, some are formed in response to wounds, and some act as part of a defense mechanism (Rowell 2012).

1.2.2 Wood structure

Differences in wood structure are not only apparent between softwoods and hardwoods, but also between species, within the stem, and within the annual rings, i.e., earlywood and latewood.

Softwood consists of 90–95% tracheids, which have a nominal diameter of approximately 35 μm and a length of approximately 3,500 μm (Siau 1995). A tracheid in earlywood has a larger diameter and thinner cell wall than one in latewood. The latewood tracheid provides stiffness and strength due to thicker cell walls, while the earlywood tracheids are used to conduct water and minerals within trees. The parenchyma cells (predominantly radial rays in softwoods) and resin canals, which contribute to the transportation and storage of water and other liquids, occupy a small fraction of volume in softwoods. The transported elements are able to flow to adjacent cells through the pits in the cell wall. Depending on their structure, the pits can be classified into three basic types: bordered, simple, and half-bordered pits (Siau 1995; Kettunen 2006). The first type is the most common and important because it interconnects two conducting cells. The overall diameter of a bordered pit chamber ranges from 6 to 30 μm in earlywood, and slightly less in latewood. The effective diameter of a pit opening is between 0.02 and 8 μm , depending on the size of the pit (Siau 1995).

Hardwoods, consisting of fibers, vessels, and parenchyma cells, have a more complex structure than softwoods. The dimensions of hardwood fibers are smaller than those of softwood tracheids. In hardwood, fibers provide mechanical support, while vessels and parenchyma cells contribute to conducting and storage (Fengel and Wegener 1989; Siau 1995). Depending on the arrangement and diameter of the vessels through the annual rings, there are diffuse porous (e.g., birch, maple, and poplar species), semi-ring-porous (e.g., walnut), and ring porous (e.g., ash, elm, and oak species) hardwood types. The diameter of vessels range from 20 to 100 μm in diffuse porous species in the temperate-zone, but they are larger in tropical conditions. In ring porous species, the diameter of vessels varies between 50 and 400 μm in earlywood and from 20 to 50 μm in latewood (Siau 1995). The number per unit volume of parenchyma cells in hardwoods is higher than in softwoods, including more rays and longitudinal parenchyma. The pits from vessels to fibers are usually bordered, while those leading to parenchyma cells are usually half-bordered or simple. Unlike softwoods, hardwood pits have no apparent opening and no thickening in the center (Siau 1995).

1.2.3 Cell wall structure

The cell wall consists of two main regions, the primary wall (P) and secondary wall (S). The major structural elements making up cell walls are cellulose microfibrils, hemicelluloses, and lignin. The middle lamella (ML) has a role as an adhesive between adjacent cells (Rowell 2012, Figure 4).

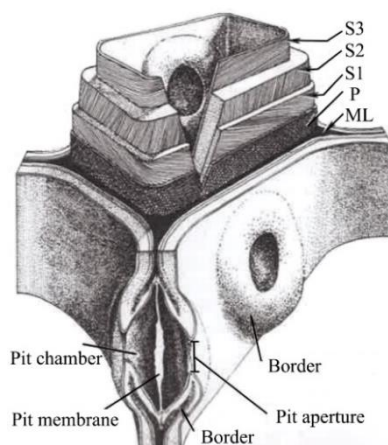


Figure 4. Simplified structure of a woody cell (reprinted [adapted] with permission from Rowell © 2012 Copyright Clearance Center).

The middle lamella is an amorphous and thin layer without any reinforcement. In the beginning of its formation, it consists of pectins containing calcium and magnesium. Later it is lignified (Kettunen 2006). The primary wall is the outermost thin layer of cell wall, where the reinforcing cellulose microfibrils are randomly oriented. The primary wall (thickness: 0.1–0.2 μm) is generally indistinguishable from the middle lamella, thus the term compound middle lamella (CML) is often used to designate the combination of adjacent primary walls and middle lamella. The thickness of CML varies from 0.1 to 0.4 μm along the wall, and the intercellular space at the corner can be 3 to 4 μm (Fengel and Wegener 1989, Rowell 2012).

The secondary cell wall is composed of three different layers interior to the primary wall. These layers can be distinguished by their orientation of microfibrils and relative distribution of wood components as outer layer (S1), middle layer (S2) and inner layer (S3) (Fengel and Wegener 1989). S1 is a thin layer (0.2–0.5 μm) characterized by a large microfibril angle (MFA) ($50\text{--}70^\circ$). S2 is the thickest secondary cell wall layer (approximately 85% of the thickness of secondary cell wall; 1–5 μm) with relatively small MFA ($5\text{--}30^\circ$). It contains a higher amount of cellulose than the other layers, and hence provides the cell wall with stiffness and strength. Therefore, the S2 layer can be considered the most important layer within the cell wall; it largely determines the physical and mechanical properties of the wood cell. The innermost layer, S3, has the lowest thickness (approximately 5% of thickness of secondary wall; 0.1–0.3 μm) and lower lignin content than other secondary cell wall layers. The S3 layer also has a relatively high microfibril angle, above 70° (Fengel and Wegener 1989, Kettunen 2006, Rowell 2012).

1.3 Water in wood

Green or fresh wood contains a large amount of water, which is located both in cell lumens and cell walls. The water in wood exists in two basic forms: bound water, which is dissolved or absorbed in cell walls, and free water, which is located as liquid in the voids (lumen, pits, cavities) within and between cells. Wood is a hygroscopic material. Thus, relative to its

environment, wet wood releases moisture to the surrounding dry air (desorption), or dry wood absorbs moisture from the surrounding humid air (adsorption). Wood's moisture content (MC) depends both on the relative humidity (RH) and temperature (T) of the surrounding air. The RH has a stronger effect than the T. If the ambient RH and T conditions are stable, wood will gradually reach its characteristic equilibrium moisture content (EMC) (Siau 1995), and keep it as long as the environmental conditions are maintained.

When wet wood is dried, i.e. desorption takes place, first all free water vaporizes and exits from the cell lumens and cavities. Not until then does the bound water start emitting from the cell walls. The MC, at which the cell wall remains saturated with bound water while all free water has been removed from the cell cavities, is referred to as fiber saturation point (FSP) (Tiemann 1906). The average FSP of wood is often assumed to be approximately 30% (Siau 1995). However, the state from which the FSP is reached (adsorption vs. desorption) also affects the FSP value. When the wood reaches the FSP from a state below 100% RH, the adsorption process in the hygroscopic region is hindered by the cellulose crystalline, lignin matrix, and the intermolecular hydrogen bonds between the cellulose chains, which are more pronounced at lower MC. Thus, the spaces for water vapor sorption between microfibrils and fibers are smaller in the hygroscopic region (Zauer et al. 2014), resulting in a smaller FSP value. In contrast, when the cell wall is saturated and fully swollen, the availability of bonding sites of sorption on molecular surfaces is higher, leading to a higher FSP value (Chen and Wangaard 1968).

Water uptake in wood is dominated by cell wall absorption in the hygroscopic range, while it is dominated by capillary condensation in pits, lumen, vessels, and other voids in the over-hygroscopic range (Thybring et al. 2018). When the MC is far below the FSP, the bound water molecules within cell walls is tightly bonded to the hydroxyl groups via hydrogen bonding (Figure 5a). The volume of bound water is limited by the number of available sorption sites for water molecules. Hemicelluloses are often recognized as the most hydrophilic components in the wood cell wall due to the abundant availability of free OH groups. The OH groups in the amorphous regions of the cellulose microfibrils are also highly accessible to water adsorption. However, the crystalline regions are mostly inaccessible to water molecules (Skaar 1988). When the MC increases towards the FSP, more water molecules are present in the cell wall, resulting in clusters of water in the cell walls (Figure 5b). When the MC is above the FSP, water will be present not only in the cell walls, but also in cell lumens (Figure 5c).

The phases of water in wood cells can be distinguished by nuclear magnetic resonance (NMR) relaxometry. Water molecules confined to pores are subjected to interactions that change the NMR relaxation times. The T_2 (spin-spin relaxation time) of liquid water depends on their mobility and local environment. For example, the assigned moisture components with shorter T_2 values (a few milliseconds) are associated with bound water in cell wall, whereas the components with longer T_2 values (dozens to hundreds of milliseconds) are associated with free water in voids, such as cell lumen or bordered pits (Labbé et al. 2002; Telkki et al. 2013; Kekkonen et al. 2014). The free water distribution can be visualized by magnetic resonance imaging (MRI). The intensity of the NMR signal is proportional to the number of hydrogen nuclei in the wood (Kekkonen et al. 2014; Javed et al. 2015).

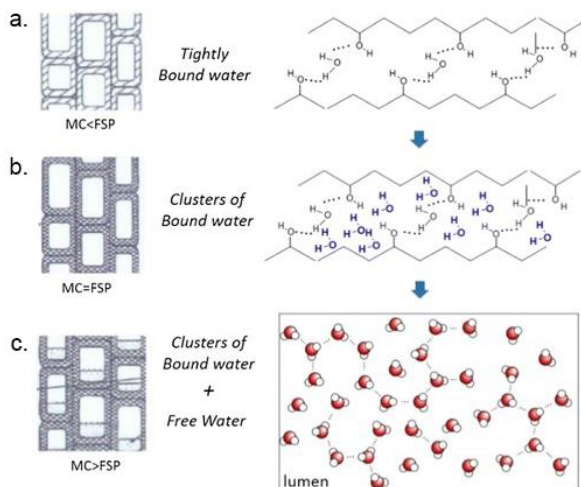


Figure 5. Schematic presentation of water in cell walls and lumens at different moisture contents (reprinted [adapted] with permission from Gezici-Koç et al. © 2017 Springer).

The melting point of water confined to a small wood cell pore is lower than that of bulk water (0 °C). According to the Gibbs-Thomson equation (Equation 1) (Jackson and Mckenna 1990), the melting point (ΔT_m) of liquid confined in a pore is inversely proportional to the radius (r) of the pore:

$$\Delta T_m = T_0 - T_m = \frac{2\sigma T_0}{r\Delta H_f \rho} = \frac{k}{r} \quad (1)$$

where, T_0 is the melting temperature of bulk liquid, T_m is the melting temperature in a cylindrical pore with a radius r , σ is solid-liquid interface energy, H_f is the bulk enthalpy of fusion, and ρ is the density of frozen water.

The melting point distribution of water confined to wood pores can be studied by measuring its ^1H NMR cryoporometry as a function of temperature to quantify the amount of liquid within different sizes of pores. On the other hand, such distribution can be converted by Equation 1 to provide information on the pore size distribution of wood (Aksnes and Kimtys 2004; Mitchell et al. 2008).

1.4 Thermal modification process

TM is a modification process designed to enhance some of the critical parameters signifying the performance of wood material in outdoor uses without using chemicals to obtain irreversible changes in its structure and properties. As a consequence of increased environmental consciousness and comparatively low processing costs, TM has developed into the most common industrial modification process to improve dimensional stability, biological durability, and thermal insulation properties of wood under varying end-use conditions since the 20th century (Hill 2006). TMW as a material is bio-degradable and can be disposed at the end of its service life by either burning or placing into the normal waste system. There are several thermal modification systems (Rapp 2001), out of which the ThermoWood® process is the most

widespread. The sales production of ThermoWood® has risen over ten times from approximately 20,000 m³ in 2001 to over 200,000 m³ in 2018 (ThermoWood Production Statistics 2018). The material used in this thesis was modified according to the ThermoWood® process.

The licensed ThermoWood process consists of three phases that for industrial lumber grades take ca. 42 hours to complete (Figure 6. ThermoWood Handbook 2003):

1) High-temperature drying

The kiln temperature is raised rapidly to a level of around 100 °C with steam. After that, the temperature is further increased steadily to 130 °C, during which time high-temperature drying takes place and the MC in wood is reduced to nearly zero before the actual thermal modification phase begins. This drying phase is important to avoid internal checks. The duration of the drying depends on the initial moisture content of the wood, wood species, and timber thickness. Raw material can be green or dried wood.

2) Thermal modification

In the thermal modification phase, the temperature is increased to 185–215 °C depending on the processing level. The target temperature is maintained constant for 2–3 hours depending on the end-use application. Steam is used during the thermal modification phase to transfer heat and to prevent the wood from burning and charring. Steam also affects the chemical changes taking place in the wood.

ThermoWood® has two standard modification classes: Thermo S (“S” stands for stability) and Thermo D (“D” stands for durability). Thermo S wood is mainly applied for furnishing and fixtures in dry conditions, whereas Thermo D wood can, for instance, be applied for cladding, decking, exterior doors, outdoor structures, and garden furniture.

3) Cooling and moisture conditioning

The temperature inside the kiln is lowered by using water spray systems. When the temperature has reached 80–90 °C, re-moisturizing takes place to bring the MC of wood to an appropriate level of 4–7% for the end use. The conditioning phase takes 5–15 hours, depending on the treatment temperature, species, and lumber dimensions.

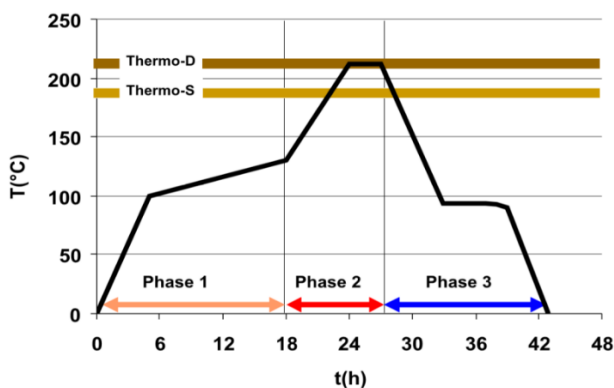


Figure 6. ThermoWood® production process (reprinted [adapted] with permission ThermoWood Handbook © 2003 ThermoWood Association).

1.5 Effects of exposure conditions on wood

1.5.1 Changes in wood due to thermal modification

Chemical changes

Hemicelluloses are the least thermally stable structural components in the wood as a result of their amorphous character and the lower degree of polymerization (Gonzalez-Peña 2009). When wood is heated, hemicelluloses degrade by dehydration with the decrease of hydroxyl groups. At the same time, hemicelluloses undergo deacetylation reactions, and the liberated organic acids such as acetic acid can further catalyze the hydrolysis of hemicelluloses to soluble sugar and depolymerize cellulose, as well, causing the formation of formaldehyde, furfural, and other aldehydes (Tjeerdsma et al. 1998; Weiland and Guyonnet 2003; Nuopponen et al. 2004). The degree of hemicellulose degradation is the greater and faster with the severity of the modification and the present moisture content (Stamm 1956; Mitchell 1988; Hill 2006; Esteves and Pereira 2009). In addition, wood species also affect its thermal degradation behavior. Since hardwoods contain a higher proportion of hemicelluloses than softwoods, they are degraded more extensively when subjected to elevated temperatures (Kamdern et al. 2002, Esteves et al. 2007).

Cellulose shows higher thermal resistance than hemicelluloses, and it is very stable up to about 165 °C (Esteves et al. 2008a; Rowell 2012; Kacik et al. 2015). Degradation of amorphous cellulose was observed when heated for 4 hours at a temperature above 185 °C (Boonstra and Tjeerdsma 2006). The thermal degradation process of cellulose is not restricted to the cleavage of molecular chains, but also dehydration and oxidation reactions take place (Fengel and Wegener 1989). Relative increase in cellulose crystallinity due to degradation of amorphous cellulose has been reported to occur during TM of wood (Bhuiyan et al. 2000, Andersson et al. 2005, Bhuiyan and Hirai 2005). Such changes in crystallinity appear to be more pronounced when wood is heated in humid conditions (Bhuiyan et al. 2000, Bhuiyan and Hirai 2005).

Lignin is the most thermally stable wood component and it degrades gradually over a wider temperature range compared to carbohydrates, due to its high structural diversity (Alén et al. 2002). The number of free reactive sites on the aromatic ring of lignin increases under heat, and cross-linking reactions occur through connecting aromatic rings by methylene bridges (Tjeerdsma et al. 1998; Nuopponen 2004). New esters are formed after modification at high temperature and the etherification of hydroxyl groups results in decreased hygroscopicity (Tjeerdsma and Militz 2005). The relative lignin content in wood increases with the severity of thermal modification as a result of hemicelluloses and cellulose degradation and lignin re-polymerization with hydrocarbon fractions from carbohydrate degradation (Avni et al. 1985, Alén et al. 2002, Nuopponen 2004, Yildiz et al. 2006).

Most of the extractives evaporate or degrade during thermal modification. As a result of degradation of cell wall structural components, new compounds can be extracted from solid wood, e.g., anhydrosugars, mannosan, galactosan, levoglucosan, and two C5 anhydrosugars, after thermal modification (Nuopponen 2003; Esteves et al. 2008b). It is considered that degradation of extractives does not significantly contribute to the mechanical performance of the wood due to these components only being present in minor proportions.

Cell wall changes

Microscopic cell wall damages occur in wood as a consequence of TM. The damage is due to wood components losses by thermal decomposition and subsequent different volume shrinkage of different cell wall layers, as well as microcracks (Fengel and Wegener 1989).

Softwoods are sensitive to tangential cracks in the latewood, especially wood with narrow annual rings and/or species with an obvious boundary between earlywood and latewood. Boonstra et al. (2006a) noticed damage to parenchyma cells in the rays and epithelial cells around resin canals in thermally modified Scots pine sapwood but not in heartwood. Hardwoods are sensitive to collapse of the vessels and deformation of the libriform fibers near to the vessels (Boonstra et al. 2006b). Broken cell walls perpendicular to the fiber's longitudinal axis, resulting in transverse ruptures, was noticed in both softwoods and hardwoods after thermal modification (Boonstra et al. 2006a,b). Destruction of tracheid walls and ray tissues results in a more open wood structure (Gosselink et al. 2004; Andersson et al. 2005). In addition, the removal of cell wall components, degradation of amorphous cellulose, and pit deaspiration increase the porosity of wood (e.g., Hietala et al. 2002; Andersson et al. 2005; Awoyemi and Jones 2011).

Changes in sawn timber properties

TM reduces the EMC and hygroscopicity of wood due to the dehydration of hydrophilic hemicellulose, increase in cellulose crystallinity, and cross-linking reaction of lignin (Tjeerdsma and Militz 2005; Hill 2006; Esteves and Pereira 2009; Sandberg et al. 2017). Wood is susceptible to decay in high humidity atmospheres. Due to the reduced hygroscopicity and EMC of wood as a result of TM, the moisture-induced biodegradation, deformation, and dimensional changes become more limited (e.g., Kamdem et al. 2002; Hill 2006; Borrega et al. 2009; Esteves and Pereira 2009). Consequently, TM increases the dimensional stability and durability of wood, which favors its uses in exterior applications.

In thermal modification, the color of wood becomes darker throughout the material. The color of modified wood is affected by the treatment temperature and time, and it is darkened with increasing modification severity (Hill 2006; Esteves and Pereira 2009). In addition, the color change is more pronounced and faster if no steam is used as a heat transfer media in the modification process (Esteves et al. 2008c). The darker color of modified wood is attributed to the formation of colored degradation products from hemicelluloses and the formation of oxidation products such as quinones during TM (Tjeerdsma et al. 1998; Sundqvist 2004).

TM has a negative effect on most mechanical properties of wood (e.g., Esteves and Pereira 2009; Heräjärvi 2009). The major reason for the loss of strength is degradation of hemicelluloses, which particularly affect the bending and tensile strength of wood (Boonstra et al. 2007; Heräjärvi 2009; Herrera-Díaz et al. 2018). The cross-linking reaction of lignin and the increase in cellulose crystallinity give a positive impact to compressive resistance parallel to the grain (Esteves et al 2008a). In contrast, Korkut et al. (2008a,b) reported that the compression strength both parallel and perpendicular to the grain decreased after TM. The hardness of wood is sometimes reported to increase (e.g., Poncsák et al. 2006; Boonstra et al. 2007) and sometimes decrease (Korkut et al. 2008a) after TM, and sometimes no difference was detected (e.g., Heräjärvi 2009) between TM and non-modified specimens.

1.5.2 Changes in wood due to moisture and liquid water

Physical and mechanical properties of wood depend closely upon its moisture content. When wood is protected from contact with liquid water, its MC changes slowly by water vapor

sorption as a function of both RH and T of the surrounding air. On the other hand, contact with liquid water can induce rapid changes in the MC of wood. The liquid water absorption can bring the MC of wood above FSP, which water vapor sorption cannot do (Siau 1995; Glass and Zelinka 2010).

Swelling and shrinkage mainly take place in cell walls, whereas the changes in lumen dimensions due to moisture changes are negligible (Siau 1995). Thus, the dimensional change of wood depends on the amount of bound water. When the MC is below the FSP, wood swells as it absorbs moisture and shrinks as it loses it. Shrinking and swelling result in warping, checking and splitting of lumber. Wood is an anisotropic material, and the dimensional changes mostly take place in a tangential direction, approximately two times more than in the radial direction, whereas the longitudinal changes are practically irrelevant in magnitude. For most species, the swelling and shrinkage in longitudinal direction is approximately 0.1–0.2% from green to oven-dry wood (Glass and Zelinka 2010). Due to the difference in swelling/shrinkage and the curvature of the annual rings, a combination of dimensional changes in radial and tangential directions results in the undesired distortion of wooden objects.

The mechanical properties of wood decrease as a result of the increase in bound water content in cell wall. This is because water molecules replace hydrogen bonding in the amorphous area of wood, which enhances the flexibility of the polymer networks and facilitates the deflection of wood during loading. Moreover, the water-induced cell wall swelling causes fewer available cell wall substances per unit area to resist the load (Kulasinski et al. 2015; Peng et al. 2016).

When wood is in contact with liquid water, a hydrolysis reaction of polysaccharides occurs easier in acidic medium than in neutral and alkaline media. Most wood species are known to be acidic in a neutral situation (Fengel and Wegener 1989). Other organic acids, such as acetic acid generated during TM, will accelerate the hydrolysis of TMW components (Tjeerdsma et al. 1998; Sundquist 2004). Acidic hydrolysis finally leads to cleavage of glycosidic bonds of glycosides, di-, oligo- and polysaccharides (Fengel and Wegener 1989). Crystalline cellulose and lignin are more resistant to hydrolysis than hemicelluloses. Hemicellulosic monosaccharides, such as xylose, mannose, and galactose, can be found after hydrolysis in diluted acid (Hoebler et al. 1989).

1.5.3 Changes in wood due to weathering

Weathering is the general term used to define the slow degradation of materials exposed to weather (e.g., Williams 2005). Wood is susceptible to degradation induced by natural factors, such as sunlight, pollutants, abrasion by windblown materials, a wide array of microorganisms, and changes in temperature and moisture. Photochemical degradation and discoloration of wood surface start immediately after being exposed to sunlight (Williams 2005). Hon and Ifju (1978) reported that UV light only penetrates 75 μm below the untreated wood surface, whereas visible light penetrates up to 200 μm . However, other degradation depths have also been reported, which may be due to differences in wood density and wavelength distribution of the UV radiation and visible light (Williams 2005).

Changes in chemistry

Lignin is the most sensitive structural wood compound when exposed to sunlight. UV radiation degrades wood structural components, mainly lignin, while visible light degrades the extractives of wood (Williams 2005). Absorption of photons by lignin leads to the formation of free radicals, and through the action of water and oxygen, formation of new chromophores

changes wood gradually into a silver gray color (Hon and Feist 1992; Tolvaj and Faix 1995; Ayadi et al. 2003; Temiz et al. 2007). Cellulose and hemicelluloses are also degraded by hydrolysis and oxidation. Depolymerization of amorphous cellulose leads to a gradual increase in cellulose crystallinity (Evans et al. 1996; Colom et al. 2003; Huang et al. 2012). During outdoor weathering, water probably hydrolyzes hemicelluloses, particularly at the exposed surface (Williams 2005). As lignin degrades, hemicelluloses become more vulnerable to hydrolysis. In addition, water washes away the water-soluble extractives and degradation products, thus leaving the wood surface rich in cellulose and hemicelluloses (Nuopponen et al. 2004; Yildiz et al. 2011).

Changes in anatomic structure

Photodegradation occurs pronouncedly in the middle lamellae due to its high lignin content both in softwoods and hardwoods. The lignin matrix binding microfibrils and fibrils are also degraded, resulting in cell wall checks and separation between the cell walls of two adjacent cells. Moreover, the micro-cracks formed on pit borders transverse to the cell axis can be observed on TMW after sunlight irradiation (Huang et al. 2012; Xing et al. 2015). With extended weathering, those degradations develop severe checking as fibrils and tracheids loosen and become detached from the surface (Williams 2005). Erosion rate of wood was reported to be higher at a 0–45° angle of exposure than at 90° angle, and higher in softwoods than in hardwoods (Williams 2005).

Changes in timber properties

As wood is weathered, loss of lignin and leaching of extractives from the surface make it more hydrophilic. With the combination of surface cracking, the hygroscopicity and wettability increase further after weathering (Williams 2005; Huang et al. 2012b).

The color of wood surface changes to silver gray with a general decrease in brightness, which is mainly due to photochemical reactions in lignin, and leaching of the degradation products such as quinones by rainwater, as well as leaching and degradation of extractives (Nuopponen et al. 2004; Xing et al. 2015; Tomak et al. 2018). Moreover, the degradation products of weathering provide nutrients for fungi and molds, which in turn promote discoloration and visual growth of microbes on the surface and lead to more severe deterioration of the structure (Eaton and Hale 1993).

Water abrades the surface also mechanically, thus causing checking and erosion (Williams 2005; Yildiz et al. 2013). Deformations, such as warping and cupping, and degradations in wood components reduce the mechanical properties after weathering (Hill 2006; Yildiz et al. 2011; Rowell 2012; Tomak et al. 2014).

TM is reported to improve the weathering resistance of wood. The decreased EMC increases the dimensional stability and durability of wood under varying relative humidity conditions (Esteves and Pereira 2009), which results in fewer checks and longer service life. The condensed lignin structure and low hygroscopicity of TMW protect it from chemical degradation and diminish the leaching of degradation products, which subsequently decrease the changes in color and surface roughness (Nuopponen et al. 2004; Temiz et al. 2006; Yildiz et al. 2011; Tomak et al. 2014). However, it is reported that such protective effect decreases gradually in long-term weathering (Huang et al. 2012; Srinivas and Pandey 2012; Xing et al. 2015).

1.6 Gaps in knowledge

TMW is a material nowadays widely used in water contact applications indoors (e.g., sauna benches and panels) or exterior applications (e.g., garden furniture, decking, cladding, window frames) where a good dimensional stability and durability are required. During its service life, moisture and other weathering factors cause changes in wood chemistry, structure, and mechanical performance, which consequently affect the product's service lifetime and maintenance need.

The effect of thermal modification on wood properties has been studied extensively (see: Hill 2006; Esteves and Pereira 2009). The weathering performance of TMW has been studied both outdoors (e.g., Sandberg 1999; Yildiz et al. 2011; Tomak et al. 2014, 2018) and in controlled laboratory conditions (e.g., Temiz et al. 2007; Huang et al. 2012, 2013; Yildiz et al. 2013; Xing et al. 2015). Based on the existing literature, the development of TMW properties in hazard class 3 conditions (standard EN 335-1 2006) is not sufficiently documented and understood. There is a need for analytical and time-dependent information and better understanding regarding the chemical, structural, and physical changes that take place in TMW as a result of frequent wetting exposure outdoors.

1.7 Research objectives

The general objective of this study was to investigate the effects of water and weather exposure on the chemical components, cellular structure, and physical properties of thermally modified Scots pine (*Pinus sylvestris*), Norway spruce (*Picea abies*) and European ash (*Fraxinus excelsior*) wood. To achieve this target, the specific objective of this work was to study the structural changes of TMW and its properties in

- 1) long-term water contact exposure: surface chemistry, pH, microstructure;
- 2) different temperature - relative humidity combinations in controlled weather chamber conditions: density, EMC, swelling and shrinkage, Brinell hardness;
- 3) natural weathering in a Nordic environment: density, surface chemistry, pH, cell wall pores, water phases distribution, FSP, EMC, color, cracking, cupping, Brinell hardness.

2 MATERIALS AND METHODS

2.1 Study materials and thermal modification

Boards of Scots pine (*Pinus sylvestris* L.), Norway spruce (*Picea abies* Karst.), and European ash (*Fraxinus excelsior*) were used as materials in this study. Quarter-sawn European ash wood and flat-sawn softwood (Norway spruce and Scots pine) contained both heartwood and sapwood. The boards were first kiln-dried at 60 °C for two weeks and then thermally modified into two classes, Thermo S and Thermo D using the commercial, industrial ThermoWood® process. The modification details are shown in Table 1.

Unmodified boards, originating from the same materials as the thermally modified ones, were used as controls. In addition, copper salt (Celcure C4, Koppers Inc., USA) impregnated Scots pine lumbers (NTR preservation class AB) with dimensions of 120 mm × 25 mm × 5000 mm (T × R × L) were bought from a lumber store to be used as a reference material.

Table 1. The dimensions and the thermal modification parameters of samples used for long-term water contact exposure test (LWC), controlled temperature - relative humidity weather chamber test (T-RH), and natural weathering test (NW)

Test	Wood type	Dimensions (T × R × L)	TM parameters		Manufactory
			Thermo S	Thermo D	
LWC	Softwood	100 × 25 × 215 mm ³	180 °C, 2 h	212 °C, 3 h	Lahti University of Applied Sciences
		100 × 50 × 215 mm ³	180 °C, 2 h	212 °C, 4 h	
T-RH	Softwood	130 × 32 × 4000 mm ³	180 °C, 2 h	212 °C, 3 h	HJT-Holz Ltd
	Hardwood	130 × 32 × 4000 mm ³	190 °C, 2.5 h	200 °C, 2.5 h	
NW	Softwood	130 × 32 × 4000 mm ³	180 °C, 2 h	212 °C, 3 h	HJT-Holz Ltd
	Hardwood	130 × 32 × 4000 mm ³	190 °C, 2.5 h	200 °C, 2.5 h	

2.2 Long-term water contact exposure test

Specimens of different species and treatments were soaked in tap water in separate compartments for a maximum of twenty weeks. Weights were used to keep the specimens completely submerged. The water was changed once a week during the first eight weeks of the test, and then at two-week intervals after eight weeks. The water changes were carried out to limit the growth of micro-organisms on the specimens and to imitate outdoor conditions where water is also changed occasionally as a result of precipitation. Measurements of Fourier transform infrared spectroscopy (FTIR), pH, and anatomy observations were carried out every two weeks (Paper I).

2.3 Controlled T-RH weather chamber test

The exposure tests were conducted using a controlled weather chamber (Convion PGW 36, Winnipeg, Man., Canada) at the University of Eastern Finland. To imitate the wet and dry end-use conditions, specimens were conditioned for several weeks first at 20 °C and 65% RH, then at 10 °C and 90% RH, and finally at 30 °C and 30% RH. The masses of three specimens from each group were measured once per week, and EMC was achieved when the two consecutive mass measures were constant. Measurements of density, EMC, swelling and shrinkage, and Brinell hardness were carried out once the equilibrium was achieved at each T-RH condition (Paper II).

2.4 Outdoor weather exposure test

Natural weathering test of modified and unmodified control boards was performed at the botanical garden, Botania, Joensuu, Finland (62°36'6" latitude, 29°43'26" longitude) from November 2016 to October 2018. The meteorological data during the weathering period are shown in Table 2. Boards were set outside without any cover from sun, rain, snow, wind, etc. To mimic conventional material uses such as decking, boards were attached parallel to the

ground (pith side upward) in a 30-mm-deep pool/basin, so that they were occasionally immersed by rainwater, snow or ice. A 2-mm-thick metal net with plastic casing (100 ×100 mm mesh size) was installed in the bottom of the pool in order to prevent the specimens from being in direct contact with the pool bottom. The boards were attached to the net with plastic cable ties to avoid flowing away when the pool became full of rainwater.

Table 2. The meteorological data for Joensuu between November 2016 and October 2018 (Sources: Finnish Meteorological Institute)

Period	7 months	12 months	19 months	24 months
Climatic parameters (monthly average)	(Nov. 2016 – May 2017)	(Jun. 2017 – Oct. 2017)	(Nov. 2017 – May 2018)	(Jun. 2018 – Oct. 2018)
Precipitation (mm)	40.8	55.8	43.2	64.8
Temperature (°C)	-2.3	11.2	-1.5	13.2
Max temperature (°C)	6	15.3	12.7	19.7
Min temperature (°C)	-6.9	3.8	-11.2	4.3
Relative humidity (%)	76.9	76.8	78.4	73.2
Cloudiness (1 to 8)	5.7	5.5	5.6	4.3
Global radiation (W/m ²)	70.9	134.3	78.1	153.8
Long wave solar radiation (W/m ²)	279	334.6	279.4	334.2
Ultraviolet irradiance (in- dex)	0.3	0.6	0.3	0.7

Density, EMC, surface chemistry, pH, color, Brinell hardness, and cupping were repeatedly measured in late May and late October of both years (Paper III). Moreover, to analyze the changes in water phases distribution, FSP, and cell wall pores, five thermally modified specimens from each species and treatment underwent NMR measurements before and after the weathering period of 24 months (Paper IV).

In addition, five boards from each species and treatment were installed vertically above ground to imitate vertical cladding. Checks were analyzed from those boards twice: before and after the two-year exposure (Paper III).

2.5 Analyses of wood specimens

2.5.1 Overview of experimental material

The dimension and number of specimens for each measurement are shown in Table 3. Knots and other visible defects were avoided when specimens were prepared.

Table 3. Dimension and number of specimens (LWC: long-term water contact test; T-RH: different temperature - relative humidity combinations test; NW: natural weathering test; C: control; S: Thermo S; D: Thermo D; I: copper salt impregnation)

Test	Measure- ment	Dimension of speci- men (mm ³) (T × R × L)	N of specimens									
			pine				spruce			ash		
			C	S	D	I	C	S	D	C	S	D
LWC	FTIR	50 × 25/50 × 10	4	12	12		5	12	12			
	pH	powder prepared from Ø 12.5 × 16 bulk wood	4	4	4		4	4	4			
	Microscopy	50 × 25 × 25	3		10							
T-RH	Basic density	130 × 32 × 20	30	30	30	30	30	30	30	30	30	30
	EMC	130 × 32 × 150	30	30	30	30	30	30	30	30	30	30
	Swelling and shrinkage	130 × 32 × 60	30	30	30	30	30	30	30	30	30	30
	Hardness	130 × 32 × 150	30	30	30	30	30	30	30	30	30	30
NW	Basic density	130 × 32 × 10	23	24	24	22	24	24	24	18	24	25
	FTIR	65 × 32 × 5	23	24	24	22	24	24	24	18	24	25
	pH	2 g wood powder	23	24	24	22	24	24	24	18	24	25
	NMR	Ø 6 × 20	5	5	5		5	5	5	5	5	5
	EMC	130 × 32 × 70	23	24	24	22	24	24	24	18	24	25
	Colour	130 × 32 × 70	23	24	24	22	24	24	24	18	24	25
	Cracking	130 × 32 × 2000	5	5	5	5	5	5	5	5	5	5
	Cupping	130 × 32 × 1000	15	15	15	11	14	17	14			
Hardness	130 × 32 × 70	23	24	24	22	24	24	24	18	24	25	

2.5.2 Chemical properties

Surface chemistry by FTIR spectroscopy

Specimens were first oven-dried at 105 °C for 24 h and stored in a desiccator to minimize the effect of ambient humidity. Then, an approximately one-mm-thick slice was cut with a knife from the pith side of the tangential surface of each specimen, and firmly pressed against the attenuated total reflection (ATR) crystal. The FTIR spectrum of each specimen was acquired as an average value of three (in LWC test) and two (in NW test) slightly different measurement positions on the up-facing pith side containing both earlywood and latewood, using FTIR-ATR (Bruker Ltd, Leipzig, Germany) with a resolution of 4 cm⁻¹ (16 scans) over the 4,000–600 cm⁻¹ wavelength range. All intensity ratios were normalized by using the peak intensity at 1,369 cm⁻¹, which corresponds to aliphatic CH stretching in CH₃ in carbohydrates and lignin (Mononen et al. 2005; Huang et al. 2013).

In addition, changes in the total crystallinity index (TCI), cellulose lateral order intensity (LOI), hydrogen bond intensity (HBI) and OH/CH₂ ratio of Scots pine and Norway spruce during the LWC test period were calculated and compared between the different treatments (Equations 2–5, Huang et al. 2012; Kacık et al. 2015). TCI and LOI reflect the degree of crystallinity in the cellulose, HBI demonstrates the strength of hydrogen bonds between wood

molecules and the OH/CH₂ ratio partly reflects the hygroscopicity of wood. The following values for these variables are presented here:

$$\text{Total crystallinity index (TCI)} = A1369/A2900, \quad (2)$$

$$\text{Cellulose lateral order intensity (LOI)} = A1423/A897, \quad (3)$$

$$\text{Hydrogen bond intensity (HBI)} = A3340/A1335, \text{ and} \quad (4)$$

$$\text{OH/CH}_2 \text{ ratio} = A3340/A2900, \quad (5)$$

where A1369 is the intensity of aliphatic CH stretching in CH₃, A2900 is the intensity of anti-symmetric and symmetric CH_n stretching, A1423 is the intensity of CH₂ symmetric bend, A897 is the intensity of anti-symmetric out-of-phase stretching plus CH deformation, A3340 is the intensity of OH stretching and A1335 is the intensity of OH in plane bending.

pH

In the LWC test, specimens of Ø 12.5 × 16 were grinded into powder using a micro-grinder (A10, IKA Corp., USA.). Then, 20 ml of Milli-Q water was added to the wood powder in a test tube. After the wood powder was thoroughly mixed with water, the pH values were measured from the solution with a pH meter (PHM 220, MeterLab, Radiometer Analytical Corp., USA).

In the NW test, specimens were grinded into fine powder using the Ultra Centrifugal Mill ZM 200 (Retsch GmbH, Haan, Germany). The solutions of 2 g wood powder in 40 ml of Milli-Q water were used for pH measurement with the Lab 860 pH meter (Schott AG, Mainz, Germany).

The pH meter was calibrated against buffers of pH 7 and pH 4 before the measurements in both tests.

2.5.3 Anatomic structure

The cross-sections of the specimens, including both heartwood and sapwood, were pre-soaked underwater for two hours and cut with a microtome before the exposure test to provide an even surface for the observations. A thin line was cut with a sharp knife on the cross-sections of the specimens to provide consistent microscopy observations that followed this line every time. An inverted materials microscope (Nikon Eclipse MA200, Japan) was used for observations at 50× magnification. The specimens were taken out of the water and air-dried in a well-ventilated room until the surface was visually dry. The structural changes were analyzed visually from the microscopy images.

2.5.4 Physical properties

Basic density

Basic density was calculated based on dry mass and green volume. Green volume was determined using the water displacement method after soaking specimens underwater for three weeks. Dry mass was measured after the specimens were oven dried at 105 °C until constant mass. Basic density was calculated by dividing the dry mass by green volume.

Equilibrium moisture content (EMC)

After the specimens were conditioned and their mass was stabilized, they were oven-dried at 105 °C until constant mass. The EMC were calculated using Equation 6:

$$\text{EMC (\%)} = \frac{m_d - m}{m_d} \times 100, \quad (6)$$

where m_d is the oven dry mass and m is the mass when EMC was achieved.

Water phases distribution, FSP and pore size distribution analyses by NMR measurements

Cylindrical specimens containing 6–13 annual rings along the axis were prepared both before and after natural weathering. The specimens were immersed in distilled water in room temperature for a period of one month to ensure full cell wall saturation before NMR measurements. The visible water from the surface of the wood specimens was removed before weighing and inserting a sample into a 10-mm medium wall NMR tube. The NMR tube was closed with a plastic cap to avoid moisture evaporation. Three NMR technologies were used in this study: *relaxometry*, *cryoporometry*, and *magnetic resonance imaging (MRI)* to investigate the water phases, pore size distribution and free water distribution, respectively.

^1H NMR *relaxometry* and *cryoporometry* measurements were carried out on a Bruker Avance III 300 spectrometer with a magnetic field strength of 7.1 T using a 10-mm BBFO probe. In both relaxometry and cryoporometry experiments, spectra were measured using a single scan CPMG (Carr-Purcell-Meiboom-Gill) pulse sequence with an echo time of 0.5 ms and 1,024 echoes. The number of accumulated scans was 64 and the experiment time was approximately 2 minutes. The length of 90° pulse was 26.5 μs and the relaxation delay was 1.5 seconds.

For *relaxometry* measurements, spectra were measured at 295 and 263 K. The relaxation time distributions of water in various wood samples were determined by performing the Laplace inversion of the CPMG data.

For *cryoporometry* analysis, CPMG data were measured at variable temperatures spanning from 194 to 290 K with a step of 2.6 K. The temperature stabilization delay was approximately one hour at 194 K, and approximately 15 minutes for the following temperature steps. The amplitude of the first echo (the echo time 0.5 ms being much longer than T_2 of ice $\sim 10 \mu\text{s}$) was assumed to be proportional to the amount of unfrozen water and used in the determination of pore size distribution. In order to avoid the temperature dependence of thermal equilibrium magnetization defined by the Curie law, the intensities of signals as a function of temperature were corrected by multiplying with a factor T/T_0 , where T is the temperature at which one particular CPMG experiment was performed, and T_0 is the maximum temperature at which the CPMG experiment was performed. The pore size distribution was determined by a least-squares fit of a model function to the integrals as described by Aksnes et al. (2001). Constant k in Equation 1 was taken to be 30 nm K (Petrov and Furo 2006), and the value of 0.6 nm was added to the calculated true pore diameter due to the presence of a non-freezing layer with a thickness of approximately 0.3–0.8 nm (Hansen et al. 1996).

Before ^1H MRI experiments, the wood specimens were wrapped in parafilm and then fixed by Teflon spacers inside the NMR tube to prevent them from rotation due to vibrations caused by the gradients. MRI experiments were carried out using a Bruker Avance DSX300 spectrometer (Billerica, MA, USA) and Bruker Avance III 300 spectrometer before and after weathering, respectively. Both spectrometers were equipped with Micro2.5 micro-imaging units with x, y, and z gradients. The MRI measurements were carried out using a 10-mm ^1H radio frequency (RF) insert and Paravision software. The images from the radial-tangential direction of wood were acquired by using a spin-echo imaging pulse sequence. A slice with a thickness of 2 mm was measured with a field-of-view (FOV) of 25 and 30 mm in read direction and 9 mm in phase direction, and with a resolution of 100 μm per pixel in both directions.

The echo time was 13.8 ms, repetition time 1.1 s, and the experiment time was approximately six minutes with four scans. The images were analyzed by MATLAB based code.

After the NMR measurements, all specimens were oven dried at 105 °C for 24 hours, and their moisture contents were determined based on the oven dry mass and wet mass after one-month water immersion. The FSP, which denotes that the cell wall remains saturated with bound water while all free water has been removed from the cell cavities, was calculated by Equation 7 (Telkki et al. 2013):

$$\text{FSP (\%)} = \text{MC} \times (S_b/S_t), \quad (7)$$

where, S_b is the integral of the bound water peak, and S_t is the total integral of the moisture peaks in the relaxation time distribution.

Swelling and shrinkage

Dimensions from the same marked positions were measured repeatedly at each equilibrium condition. Thickness, width, and length were measured and analyzed from three, two, and three positions, respectively, as shown in Figure 7.

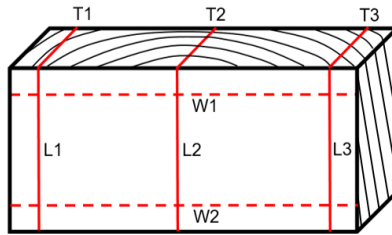


Figure 7. Dimension measurement positions in specimens (T: thickness, W: width, L: length).

Changes in tangential (T1, T3, W1, W2), radial (T2), and longitudinal (L1, L2, L3) directions were compared in terms of relative swelling or shrinkage using Equation 8. Due to the characteristic of quarter sawing, ash specimens were only analyzed regarding changes in thickness, width, and length directions:

$$\text{Relative swelling or shrinkage (\%)} = \left(\frac{\text{changes in dimension}}{\text{final dimension}} \right) \times 100, \quad (8)$$

Brinell hardness

Hardness test was carried out on the pith side in accordance with standard EN 1534 (2010). The Brinell hardness value (HB) was calculated using Equation 9:

$$\text{HB} = \frac{2 \times F}{\pi \times D \times (D - \sqrt{D^2 - d^2})}, \quad (9)$$

where F is the force applied (N), D is the diameter of the steel ball (mm) and d is the diameter of the residual indentation (mm) on the specimen surface.

Each specimen was measured three times at three different positions on the pith side. Earlywood-latewood differences and annual ring or grain patterns were not considered when selecting the position of the hardness measurement.

Color

Samples were conditioned in a climate chamber (Convion PGW 36, Winnipeg, Man., Canada) at 20 °C, 65% RH until constant mass before measurement. Color was measured over an 8-mm-diameter spot with six different measurements along the tangential direction of specimens' pith side using a spectrometer (CM -2600d, Konica Minolta, USA). The data of reflectance spectra between 360 and 740 nm wavelength range was converted to CIE L*a*b color coordinates. The negative and positive changes in L*, a* and b* values show a tendency of color to become darker and brighter, greenish and reddish, and bluish and yellowish, respectively. The total color difference (ΔE) was calculated according to the Equation 10:

$$\Delta E = \sqrt{(L_a^* - L_b^*)^2 + (a_a^* - a_b^*)^2 + (b_a^* - b_b^*)^2}, \quad (10)$$

where the subscript "a" and "b" represent the values after and before the exposure test.

Cracking

Air-coupled ultrasound (ACU) was used to evaluate the internal checking caused by weathering. The length and the position of cracked zones in a board were measured using a non-contact Puumit crack detector (Puumit Oy, Kuopio, Finland). The detection limit of checks was 10 mm. Before natural weathering, two ACU measurements were conducted: one vertical (200 kHz) and one horizontal (100 kHz, Figure 8). Two pairs of commercial Ultrat NCG200-D25 (The Ultrat Group, State College, PA, USA) sensors were used in the vertical measurement. An Ultrat NCG100-D50-P150 sensor was used as a transmitter and Ultrat NCG100-D25 as a receiver in horizontal measurement. After the two-year weathering period, the boards were conditioned indoors and ACU measurements were conducted again. Two vertical (200 kHz) and one horizontal (100 kHz) ACU measurements were conducted.

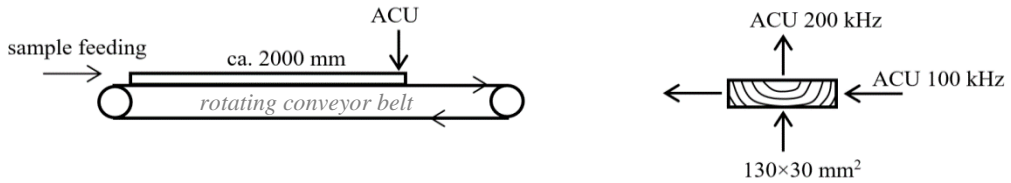


Figure 8. Setup of ACU measurements.

Cupping

For the cupping measurement, the width (Figure 9) and planer deviation were measured from the end and the middle of the boards. The average cupping values from those two positions were converted into curvature results using Equation 11 and 12:

$$R^2 = (R - D)^2 + (W/2)^2, \quad (11)$$

$$C = \frac{1}{R} = \frac{8D}{W^2 + 4D^2}, \quad (12)$$

where C is the curvature (m^{-1}), R is the radius of curvature (m), D is the planer deviation (m), and W is the width of the board (m). Because the ash boards were quarter-sawn, cupping was measured only from pine and spruce specimens.

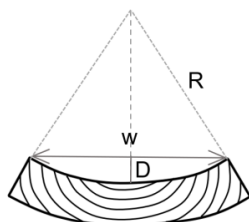


Figure 9. Cupping measurement. R, D and W represent the radius of curvature, width of the board and the planer deviation, respectively.

3 RESULTS AND DISCUSSION

3.1 Changes of wood due to moisture and liquid water exposure

3.1.1 Chemical composition and pH of wood (Paper I)

Surface chemical composition

Figure 10 presents the chemical structure of wood surface layer after the LWC test, based on FTIR-ATR spectroscopy. The intensity of a band at $1,729\text{ cm}^{-1}$ (C=O stretching in acetyl or carbonyl in hemicellulose) decreased visibly/notably in all the specimens after 14 weeks of soaking; the control specimens showed slightly larger declines than the modified ones. This change depicts the degradation of hemicelluloses (Kocaefe et al. 2008; Yildiz et al. 2011) and leaching of the degradation products during soaking. The lower degradation degree of hemicellulose in the modified wood compared to the control wood may be due to the lower initial hemicellulose concentrations in the TMW.

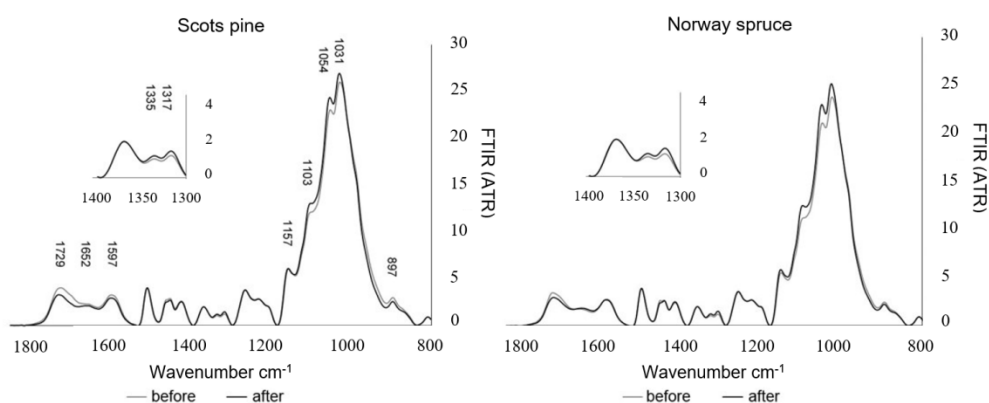


Figure 10. FTIR-ATR spectra of thermally modified (Thermo D) Scots pine and Norway spruce wood before (grey) and after (black) soaking for 14 weeks (reprinted [adapted] with permission from Paper I © 2018 Springer).

A slight signal reduction was observed at $1,652\text{ cm}^{-1}$ for the modified pine. It is likely due to the alteration of ether linkages into aromatic carbonyl structures in lignin (Hon and Shirai-shi 2001). The $1,597\text{ cm}^{-1}$ band, which corresponds to the aromatic structure of lignin, had a more evident decrease in pine wood than in spruce wood. The decreasing bands at $1,335\text{ cm}^{-1}$ (OH in plane bending) and $1,317\text{ cm}^{-1}$ (C–H vibration in cellulose) indicate changes in cellulose structure and decrease in cellulose crystallinity after soaking. The increasing intensity at $1,103\text{ cm}^{-1}$, $1,054\text{ cm}^{-1}$ and $1,031\text{ cm}^{-1}$ of all the specimens, which refer to the C–O and C=O bonds in the cellulose, indicate the increased concentrations of the alcohol and/or carboxyl groups in cellulose (Kocaeft et al. 2008). The band at 897 cm^{-1} , corresponding to the C–H group vibration of cellulose and hemicelluloses, decreased in all specimens, indicating the degradation of polysaccharides (Yildiz et al. 2011) after LWC test.

Most modified and control specimens indicated an increase in TCI and LOI values after LWC tests, suggesting an increase in the degree of cellulose crystallinity. This is possibly caused by the partial reorganization of the cellulose molecules during the soaking and oven-drying process prior to the FTIR analysis. Furthermore, the mostly decreased HBI values and increased OH/CH₂ ratios indicate weaker bonds between the molecules and higher hygroscopicity of both the modified and control wood specimens after 14 weeks of soaking.

pH

TMW specimens had lower pH value than controls, indicating the generation of acids during TM (Fengel and Wegener 1989). However, Thermo D modification resulted in lower acidity than Thermo S, which is likely caused by the fact that the ThermoWood® process was carried out in an open system, in which the organic acids liberated by thermal degradation become largely volatile and emitted from the reactor (Hill 2006; Borrega and Kärenlampi 2008; Altgen and Militz 2015). In addition, Thermo D generates more organic acids and increases the cell wall corrosion, which facilitates gas permeability (Booker and Evans 1994; Ahmed et al. 2013). Thus, the higher emissions of volatile acids consequently decrease the acidity of Thermo D wood in comparison to Thermo S wood. This trend (pH value: control > Thermo D > Thermo S) was also observed during the soaking period of the LWC test. However, the within-treatment differences over the entire soaking period were insignificant, indicating no changes in wood acidity during the LWC test.

3.1.2 Microstructure (Paper I)

Before the LWC test, a few visible cracks and holes were observed in the cell walls of TMW, which were caused by the anisotropic shrinkage of the cell-wall layers, and the degradation of the chemical components (mainly hemicelluloses) during the TM (Fengel and Wegener 1989; Andersson et al. 2005).

During the LWC test, the cell-wall degradation in the TMW occurred earlier and to a greater extent than in the control specimens (Figure 11). This is likely because TMW contains less hemicellulose; thus it has a more brittle structure, and the formation of acids during TM might promote the degradation of the cell-wall compounds during soaking (Boonstra and Tjeerdsma 2006). The thermally modified sapwood showed more evident degradation than the heartwood, which could be explained by the greater and quicker moisture uptake in sapwood (Metsä-Kortelainen et al. 2006), and subsequently greater effect in the wet stage for the sapwood than for the heartwood. Water soaking apparently increased the size and number of holes in the cell walls, which might be explained by the leaching of the water-soluble wood components, and/or hydrolysis of carbohydrates.

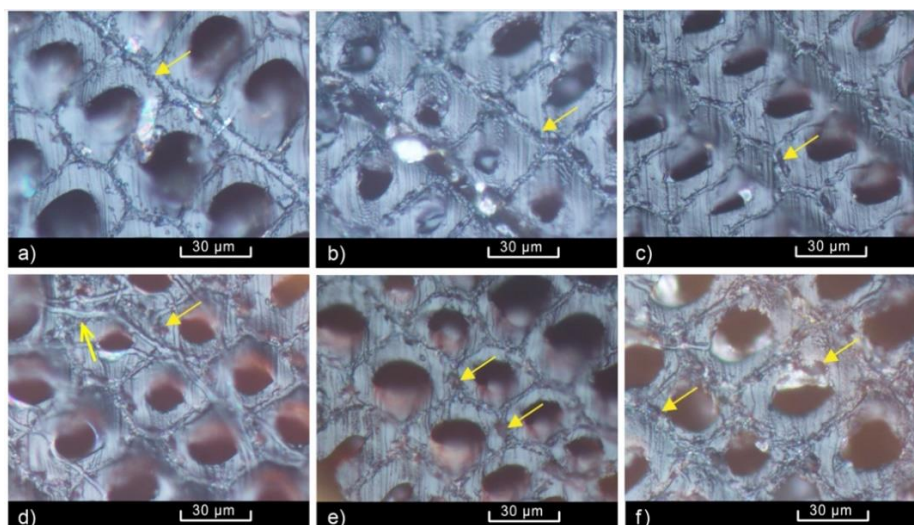


Figure 11. Cell wall structure of the Thermo D-modified Scots pine sapwood at different soaking periods; a) 2 weeks, b) 4 weeks, c) 6 weeks, d) 8 weeks, e) 12 weeks, f) 20 weeks. ↑ refers to hyphae, ↓ refers to cell wall degradation (reprinted [adapted] with permission from Paper I © 2018 Springer).

Fungal hyphae were observed on the surface of all specimens during test, which indicates that microbial degradation may also play a role in the cell-wall changes. To simulate “normal” wood in practice, specimen contamination with microbes during the storage or transportation before the tests is possible, because it was not particularly avoided.

3.1.3 EMC, swelling, and shrinkage (Paper II)

Increase in TM intensity significantly decreased the EMC for all species in all exposure conditions. This is due to the decreased hygroscopicity of wood treated in elevated temperature (Altgen et al. 2016). In addition, TM decreased the EMC more in normal climate condition (20 °C, 65% RH) than in drier (30 °C, 30% RH) or more humid conditions (10 °C, 90% RH). The EMC of impregnated pine specimens was equal to or higher than that of control specimens in all conditions.

The relative changes in tangential, radial, and longitudinal directions between different exposure conditions for pine and spruce are presented in Table 4. The results show that the moisture-dependent dimensional changes of wood are higher in the tangential direction than in the radial direction, and changes in longitudinal direction are considerably small. TM significantly reduced the swelling and shrinkage in all directions, and the reduction (especially in the tangential direction) was positively correlated with TM severity. This is due to the breakdown of the hydrophilic hemicelluloses and crosslinking of the lignin, which, subsequently, reduced the hygroscopicity of wood (Akgül et al. 2007, Ahmed and Moren 2012, Sandberg et al. 2017). On the other hand, copper salt-impregnated pine had a similar tendency of changes compared to unmodified pine, indicating no improvement in dimensional stability.

Table 4. Relative changes in tangential, radial, and longitudinal directions (unit: %, values in parentheses represent standard deviation, C: control, S: Thermo S, D: Thermo D, I: copper salt impregnated. Reprinted [adapted] with permission from Paper II © 2019 Copyright Clearance Center)

Species	Spruce			Pine			
Treatment	C	S	D	C	S	D	I
Average MC change from T20 RH65 to T10 RH90 (swelling)							
	6.01	5.86	4.90	6.00	8.75	7.21	7.56
Dimensional change, %							
Tangential	2.52 (0.23)	1.74 (0.35)	1.54 (0.29)	1.88 (0.26)	1.80 (0.23)	1.65 (0.25)	1.80 (0.26)
Radial	1.56 (0.41)	0.72 (0.26)	0.72 (0.26)	0.93 (0.31)	0.52 (0.32)	0.45 (0.30)	0.81 (0.21)
Longitudinal	0.18 (0.08)	0.03 (0.05)	0.02 (0.05)	0.13 (0.09)	0.04 (0.02)	0.02 (0.04)	0.20 (0.09)
Average MC change from T10 RH90 to T30 RH30 (shrinkage)							
	-13.17	-8.22	-6.86	-13.28	-10.89	-9.04	-14.10
Dimensional change, %							
Tangential	-4.26 (0.44)	-2.66 (0.39)	-2.35 (0.29)	-3.82 (0.40)	-2.78 (0.33)	-2.37 (0.22)	-3.76 (0.46)
Radial	-2.55 (0.43)	-1.34 (0.25)	-1.29 (0.23)	-2.03 (0.41)	-1.16 (0.27)	-1.04 (0.28)	-1.80 (0.34)
Longitudinal	-0.22 (0.08)	-0.19 (0.05)	-0.14 (0.05)	-0.21 (0.07)	-0.12 (0.04)	-0.10 (0.03)	-0.26 (0.09)

Despite the improvements in dimensional stability, the anisotropic character of swelling and shrinkage remained for the TMW. Before TM, the changes in the tangential direction were approximately 1.6 and 2.2 times greater than in the radial direction for Norway spruce and Scots pine, respectively. After the TM process, the ratio of tangential to radial changes increased up to 2.2 and 1.9 times for Thermo S and Thermo D-modified spruce and 2.9 times for modified pine, respectively. This result differs from the finding of Esteves et al. (2007b), who concluded that the TM improved the dimensional stability more in the tangential direction than in the radial direction. Apparently, the differences in thermal modification processes, wood species, and preparation of specimens between this study and the previous ones may explain the different findings. On the other hand, there are no obvious anatomical or physical explanations for the differences observed.

The relative swelling and shrinkage in directions of thickness, width, and length were calculated for all three species. The flat sawn spruce and pine indicated a dimensional change 1.5 times higher in the thickness direction than in the width direction, while quarter sawn ash boards had no difference between the two directions.

3.1.4 Brinell hardness (Paper II)

Brinell hardness correlated positively with the basic density and negatively with the EMC. The result shows that different treatments (Thermo S, Thermo D, and impregnation) did not

differ in terms of basic density and Brinell hardness within the same species at 20 °C and 65% RH and 30 °C and 30% RH (except for Thermo D-modified ash). However, at 10 °C and 90% RH, the difference between TMW and unmodified control was significant for all three species. Still, no difference between Thermo S and Thermo D specimens was observed in any species. The differences between thermally modified and control specimens were 12%, 14.4%, and 17.3% for pine, spruce, and ash, respectively. The reason for the decrease in hardness with increasing EMC is related to the fact that water replaces hydrogen bonding in the amorphous region of wood, which increases the flexibility of the polymer network and facilitates the deformation of cell walls and tissue during loading. In addition, the cell wall swelling caused by moisture uptake results in less cell wall substances per unit area to resist the load (Kulasinski et al. 2015; Peng et al. 2016).

3.2 Changes in wood due to natural weathering

3.2.1 Chemical composition and pH of wood (Paper III)

Surface chemical composition

Figure 12 shows the changes in functional groups of modified and unmodified wood between the bands of 1,800 cm^{-1} and 700 cm^{-1} during natural weathering. The signal intensity at around 3,340 cm^{-1} (OH groups in wood's polymers) increased slightly for all specimens after the weathering. It indicates increased accessibility of water, which subsequently increased the hygroscopicity of wood (Herrera et al. 2014). A reduction of the carbonyl absorption peak at 1,727–1,729 cm^{-1} was detected in all samples after weathering, which was interpreted as degradation of hemicelluloses.

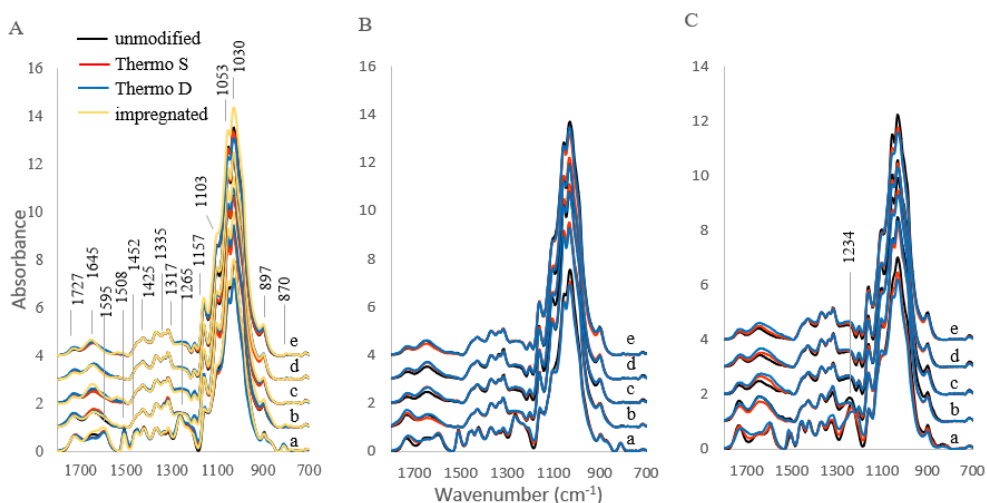


Figure 12. FTIR spectra of (A) Scots pine, (B) Norway spruce, and (C) European ash during natural weathering. The weathering period in each case is (a) 0 month, (b) 7 months, (c) 12 months, (d) 19 months, (e) 24 months.

Inconsistent changes were observed for all specimens during the weathering period at $1,645\text{ cm}^{-1}$, which is assigned to the H-O-H deformation vibration of absorbed water and formation of quinines and quinone methides. Huang et al. (2013) reported that the intensity of this band first increases and then decreases, which might be due to the formation of quinines and quinone methides (responsible for the yellowing of wood surface) resulting from exposure to UV irradiation, while the decrease is related to the leaching of these products by water.

The intensity of lignin peaks at around $1,595\text{ cm}^{-1}$ (aromatic C=C bond stretching), $1,508\text{ cm}^{-1}$ (aromatic C=C bond stretching), $1,452\text{ cm}^{-1}$ (anti-symmetric CH deformations), $1,265\text{ cm}^{-1}$ (guaiacyl unit), $1,234\text{ cm}^{-1}$ (syringyl unit) and 870 cm^{-1} (CH out of plane bending vibration) were clearly decreased or even disappeared for both modified and unmodified samples of all wood species after the first seven months of weathering. In accordance with previous studies (Yildiz et al. 2013; Tomak et al. 2018), this phenomenon indicates a rapid degradation of lignin by UV radiation. Although TMW showed slightly higher intensity at those lignin bands at the end of the test, it seems that TM cannot restrict lignin degradation after long-term weathering.

Bands at $1,335\text{ cm}^{-1}$ and $1,317\text{ cm}^{-1}$, which are primarily assigned to the cellulose component, and is related to the content in crystallized cellulose I and amorphous cellulose (Colom et al. 2003), increased at the beginning of weathering, indicating the depolymerization of amorphous cellulose and increase in cellulose crystallinity (Colom et al. 2003; Huang et al. 2012). However, the intensity of these peaks slightly decreased afterwards, which indicates that the crystalline cellulose is also degraded after longer weathering exposure (Huang et al. 2013). The increasing intensities at $1,157\text{ cm}^{-1}$ (C-O-C vibration), $1,103\text{ cm}^{-1}$ (C-O and C=C stretching), $1,053\text{ cm}^{-1}$ (C-O stretching), $1,030\text{ cm}^{-1}$ (C-O and C=O stretching) and 897 cm^{-1} (C-H vibration) after weathering were mainly related to celluloses and to a smaller extent to hemicelluloses. The increase in intensity of these peaks is clearly accompanied with the delignification of wood surface caused by photodegradation that decreases the lignin content, and thus increases the relative share of cellulose in wood. In addition, rain or wind remove the decomposition products from the surface of wood and leave the wood surface rich in cellulose (Yildiz et al. 2013).

In summary, TMW had less changes in carboxyl group (in hemicellulose), guaiacyl/syringyl ring (in lignin) and CO stretching (in cellulose) than unmodified wood. In addition, Thermo D showed less change than Thermo S. The reason for smaller changes might be related to the initially lower hemicellulose content and more stable crosslinking structure of lignin in TMW (Nuopponen et al. 2004). Copper salt-impregnated pine showed less changes in carboxyl group (hemicellulose) and aromatic C=C bond (lignin), and more increase in CO stretching (cellulose) compared to unmodified wood. However, similar changes in peak intensities responsible for the lignin, hemicellulose, and cellulose were observed on both modified and unmodified wood for all species after weathering. This indicates that TM provided limited protection of wood surface for long-term natural weather exposure, which is in accordance with previous studies (Xing et al. 2015, Tomak et al. 2018).

pH

The initial pH values of different treatments were in the order: impregnation > Thermo D > Thermo S. However, different from the previous result in the LWC test (Chapter 3.1.1), the pH value of Thermo D specimens was higher than or equal to that of controls. The difference might be related to acid formation due to different parameters used between laboratory-based (Paper I) and industrial (Paper III) modification processes, or it can be due to real differences in wood materials.

The decreasing carbonyl content due to weathering is supposed to increase the pH value. However, the weather just before each measurement day, such as rainfall and the acidity of rainwater, may also have affected the pH value. Therefore, no consistent trend in pH changes was observed during the entire exposure period.

3.2.2 Pore size distribution in cell walls (Paper IV)

The pore size distribution in cell walls calculated by the Gibbs-Thomson equation (Equation 1) is shown in Figure 13. The diameter of the pores in cell walls is mostly between 1.2–5 nm. This is in agreement with Hill (2006) and Kekkonen et al. (2014), who reported that the maximum diameter of a cell wall pore is 2–4 nm by solute exclusion method and 1.5–4.5 nm by the cryoporometry method. In the present study, approximately 60–80% of the pores with a diameter smaller than 2.5 nm refer to bound water sites (Kekkonen et al. 2014; Gao et al. 2015). The other pores with a diameter larger than 2.5 nm refer to the small void spaces, where the clusters of bound water are condensed between cellulose chains and microfibrils in cell walls (Książczak et al. 2003; Gezici-Koç et al. 2017).

The number of cell wall pores decreased with the increasing modification intensity. Weathering increased the porosity of cell walls (integral of curves) slightly in all samples (except Thermo S-modified spruce), indicating photodegradation and leaching of cell wall constituents, particularly lignin, and better accessibility of water (Ayadi et al. 2003; Temiz et al. 2007). It was surprising to find that the number of bound water sites increased, and the number of small voids decreased in pine and spruce after weathering, while ash showed the opposite result. This phenomenon might indicate that the swelling of cell wall is caused by a random absorption of water in bound water sites and small voids. However, due to the variation between the specimens before and after weathering, no definite conclusion can be drawn on this without further examination.

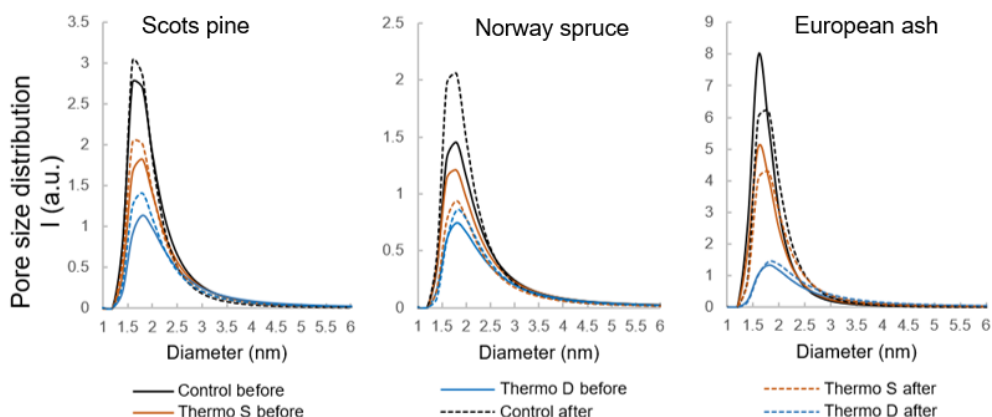


Figure 13. The pore size distribution of cell walls before and after weathering measured by NMR cryoporometry (reprinted [adapted] with permission from Paper IV © 2020 Springer).

3.2.3 Wood-water interaction (Papers III and IV)

EMC

Although the higher TM intensity resulted in lower EMC for all species throughout the exposure period, an increase in EMC during weathering was observed in all specimens (Figure 14). This is in agreement with the finding of Tomak et al. (2014). In comparison to untreated control and impregnated specimens, TMW had a more rapid increase in EMC during the first seven months, after which it normalized. On the other hand, the EMC increment rate of control and copper salt-impregnated specimens appears to accelerate as a function of time.

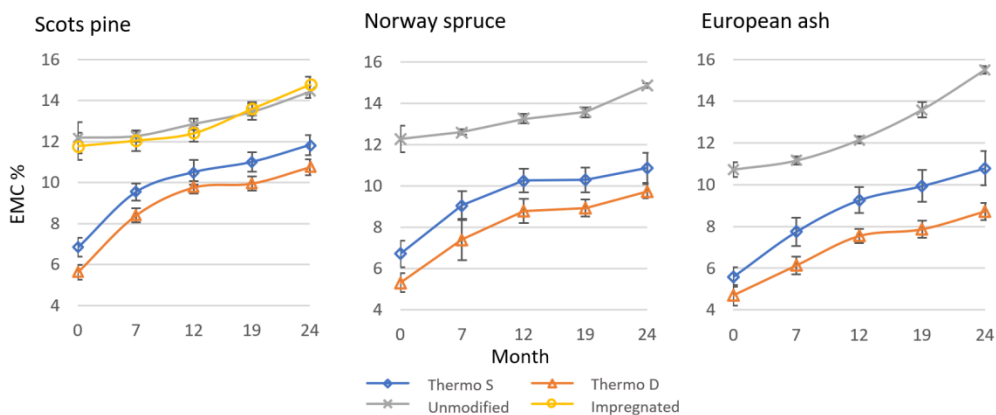


Figure 14. The EMC of modified and unmodified specimens in 20 °C and 65% RH as a function of weathering time.

Water phase distribution

Figure 15 presents the bound and free water distribution in specimens before and after weathering. At 263 K, only one T_2 signal was observed. This signal has been assigned to bound water in cell wall, because free water is frozen and its signal disappears at this temperature (Telkki et al. 2013; Fredriksson and Thygesen 2017). For pine and spruce, the T_2 values were slightly shorter than 1 ms, and they did not vary much due to TM or weathering. For ash, the initial T_2 value (around 2–3 ms) of unmodified specimens was shorter than TMW specimens (Thermo S: 1.5 ms, Thermo D: 1.1 ms), which is a result of decreased mobility of water molecules in cell walls (Gao et al. 2015; Gezici-Koç et al. 2017) of TMW. However, natural weathering did not change the T_2 value of bound water signal.

For pine and spruce at 295 K, the shortest T_2 peak (peak 1) corresponds to the bound water signal, while the other peaks arise from the free water. Peak 2 has been assigned to water in latewood tracheid lumens and ray lumens, and peak 3 was attributed to water in earlywood tracheid lumens (Kekkonen et al. 2014; Gao et al. 2015; Gezici-Koç et al. 2017). However, a different interpretation was reported by Fredriksson and Thygesen (2017), who studied the phases of water in earlywood and latewood separately and concluded that peak 3 represents lumen water in tracheid cells, while peak 2 corresponds to the free water in smaller voids, e.g., ray cell lumen, pits, and tracheid lumen ends. In addition, peak 4 has been assigned to

organic components (Labbé et al. 2006) and surface water on the specimens (Fredriksson and Thygesen 2017). After the two-year natural weathering period, peak 4 became smaller, indicating the leaching of extractives and resin. The increased T_2 values of peaks 2 and 3 implied the degradation of middle lamellae, checking of cell wall, and degradation of bordered pits by weathering (Huang et al. 2012c). More obvious changes occurred in TMW than in unmodified control specimens, and more severe modification resulted in greater changes after weathering.

For ash specimens, peaks 1, 5, and 6 at 295 K were attributed to the bound water in cell walls, free water in lumens of fibers and parenchyma, as well as free water from vessels, respectively (see: Almeida et al. 2007; Gao et al. 2015). TM splits peak 5 into more peaks, which is likely due to the pearling phenomenon (a drawback of the method that tends to split up intrinsically broad peaks into a series of narrow peaks) (Telkki 2018). However, unlike in pine and spruce, two-year natural weathering had no effect on the T_2 values in ash, but only decreased the number of peaks of Thermo S-modified specimens, indicating faster free water exchange in cell walls after weathering.

According to the spatial distribution of free water from MRI measurement, the signal arising from earlywood was more intense than that of latewood in all wet specimens. This is reasoned by the fact that free water concentration is higher in the earlywood due to greater lumen volume proportion of the tracheid cells and vessels (Kollmann & Côté 1968). The MRI results also provide evidence that natural weathering increases the water absorption independently of the treatment method, and more severe thermal modification results in better water resistance/lower hygroscopicity than milder modification both before and after the weathering.

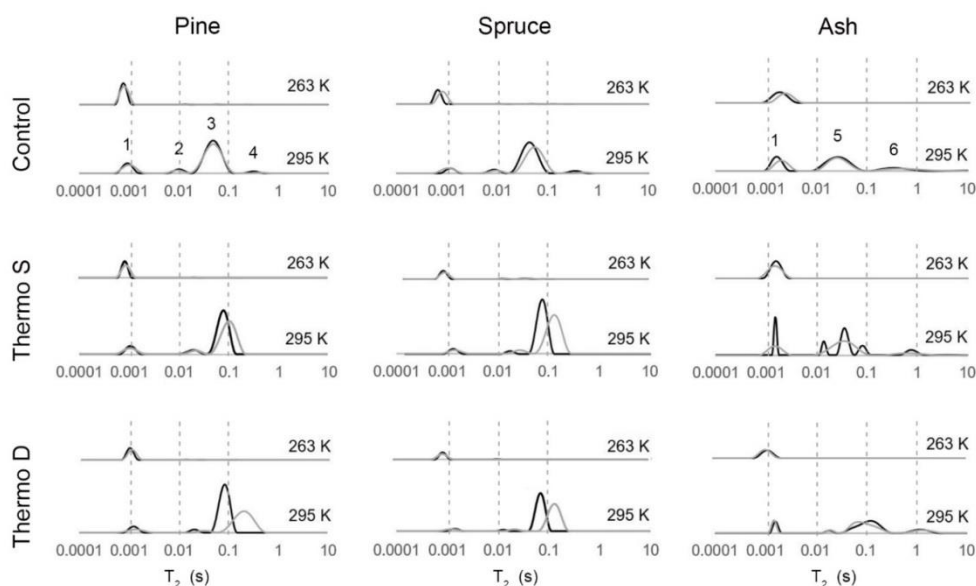


Figure 15. T_2 relaxation time distribution of samples measured by NMR relaxometry at 263 K and 295 K before (black) and after (grey) two-year natural weathering (reprinted [adapted] with permission from Paper IV © 2020 Springer).

FSP

It is reported that the FSP measured from saturated wood is higher than from wood conditioned in hygroscopic region due to the sorption hysteresis (Zauer et al. 2014, Fredriksson and Thybring 2019). According to the results shown in Table 5, the FSP values of unmodified pine and spruce were $39\% \pm 1\%$ and $38\% \pm 2\%$, respectively, which are close to the previous studies (e.g., Kekkonen et al. 2014; Gao et al. 2015). The Thermo S and Thermo D modifications decreased the FSP by 18–20% and 36–52%, respectively, and around 2–5% increase in FSP was observed in both modified and unmodified specimens after weathering. This may be caused by increased wettability due to a) reducing or removing the water repellent effect of extractives (Kalnins and Feist 1993); b) degradation of the hydrophobic lignin component (Yildiz et al. 2013; Tomak et al. 2018); and c) easier entrance of water molecules into the cell wall due to microcrack formation (Huang et al. 2012b).

Table 5. The average fiber saturation point (FSP) of specimens before and after two-year natural weathering (unit: %, C: control, S: Thermo S, D: Thermo D. Reprinted [adapted] with permission from Paper IV © 2020 Springer).

Species	Scots pine			Norway spruce			European ash		
	C	S	D	C	S	D	C	S	D
Before	38.6±0.9	30.7±1.2	24.2±1.4	37.7±1.7	31.3±3.4	24.3±3.0	47.7±1.2	37.8±3.9	22.6±0.9
After	40.4±0.5	34.6±3.4	29.9±2.0	40.7±2.0	30.7±2.0	27.3±1.6	50.6±2.6	39.4±3.4	24.5±1.5

Although the FSP increased after weathering, the decreasing trend from unmodified controls to Thermo S and Thermo D specimens indicated that TM still limits water absorption after two years of weathering.

3.2.4 Wood appearance (Paper III)

Color

It was found that TMW became darker with increasing modification temperature and time. TM increased the reddish and yellowish color in pine, spruce, and Thermo S-modified ash, but increased the reddish and bluish color in Thermo D-modified ash. On the other hand, the copper salt impregnation significantly increased the greenish color of pine.

The surface color of TMW turned towards green and blue during natural weathering. The initial dark color first lightened, and then turned darker again after seven months. The surface color of unmodified wood and copper salt-impregnated pine constantly darkened. They first became more reddish and yellowish, and then turned rapidly towards greenish and bluish after seven months. Some fluctuation in color change was observed between 12 and 24 months, which may be caused by the loss of the uppermost surface by weathering. The experimental test setup differed from ordinary end-use conditions, since the specimens were not surface treated.

The most rapid total color change (ΔE) took place in specimens during the first 12 months (Figure 16) of weathering. TMW had smaller ΔE than unmodified control specimens, and copper salt-impregnated pine had the lowest ΔE . In case of pine and spruce, increase in the intensity of modification decreased the total color change during the test, while the opposite

result was observed in the case of ash. The color changes during natural weathering are mainly due to: a) photochemical reactions in lignin and then leaching of the degradation products such as quinones by rainwater (Nuopponen et al. 2004; Tomak et al. 2018); b) transportation and degradation of extractives especially for unmodified wood (Xing et al. 2015); and c) accumulated impurities from air and rainwater and discoloration by biological organisms and mold (Tomak et al. 2014, 2018). The smaller color change of TMW could be due to the condensed lignin structure and low hygroscopicity, which diminish the leaching of degradation products (Nuopponen et al. 2004; Huang et al. 2012). The color stability of copper salt-impregnated wood against weathering might be due to a reaction of copper salt with phenolic groups of lignin to form a phenolate, which retards the formation of phenoxy radicals that contribute to color change (Deka et al. 2008).

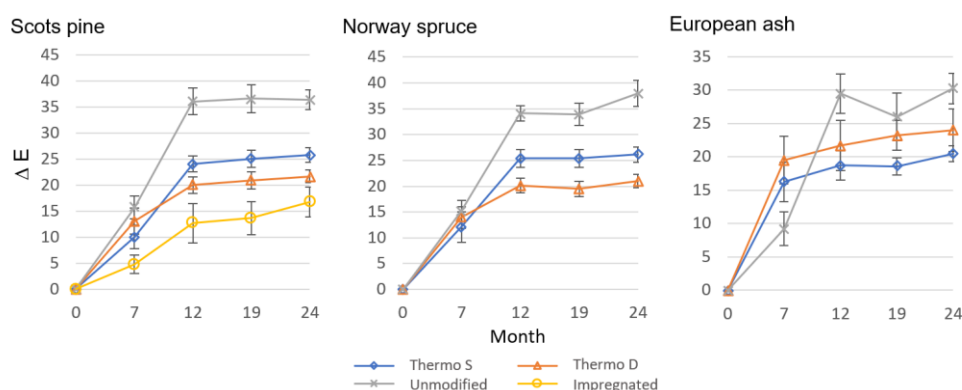


Figure 16. Changes in color of thermally modified wood during 24-month natural weathering.

Cracking

Weathering generated new checks and increased the length of the initial checks. TMW had more checks than unmodified wood after weathering in all species, and more checks were detected in Scots pine than in Norway spruce and European ash. Thermo D-modified softwood specimens had more checks than Thermo S specimens after weathering. On the other hand, copper salt-impregnated pine had less new checks than thermally modified pine. The experimental test setup differed from ordinary end-use conditions, since the specimens were not surface treated.

Different checking performance between TMW and unmodified wood has been observed previously. Vernois (2001) stated that TMW produced by Retification and "Bois Perdue" processes reduced the cracks caused by swelling and shrinkage behavior. In contrast, Feist and Sell (1987) found that weathering caused more cracks in thermally modified than unmodified spruce, while thermally modified beech had little noticeable differences in cracking compared to unmodified beech. Moreover, Jämsä et al. (2000), who modified pine and spruce by the ThermoWood process, reported that TM did not prevent cracking during weathering. The differences between findings are apparently related to the wood species, modification processes, and weathering conditions. Due to the limitation of the detector, this study did not take into account the cracks smaller than 10 mm. However, our analysis confirmed the applicability of the ACU method to detect cracks in case of TMT.

Cupping

Cupping was observed in all specimens during the 24 months of weathering. Since, cupping is caused by anisotropic swelling efficiency in the radial and tangential directions, it is affected by wood's MC, the ambient relative humidity and precipitation before each measurement day. A significant reducing effect of TM on cupping was only observed when the MC of unmodified and modified samples was above 44% and 30%, respectively. This result indicates that TM limits the cupping in wet conditions. Furthermore, Thermo D modification resulted in lower cupping deformation than Thermo S modification. This can be explained by the lower hygroscopicity and improved dimensional stability of TMW (Esteves et al. 2007b; Priadi and Hiziroglu 2013). Copper salt impregnation did not limit cupping in comparison to unmodified wood. The experimental test setup differed from ordinary end-use conditions, since the specimens were not surface treated.

3.2.5 Basic density and Brinell hardness (Paper III)

The two-year weathering did not cause significant decrease in specimen density regardless of the treatments (Table 6), which indicates no severe decay of wood.

Table 7 shows that there were no differences among Brinell hardness of thermally modified, unmodified, and copper salt-impregnated specimens of Scots pine and Norway spruce at each measurement phase during weathering. Although Thermo D ash had initially lower hardness than Thermo S and unmodified ash, the difference disappeared after weathering of 12 and 24 months.

The slight decrease in Brinell hardness of wood as a function of weathering time could be related to surface wearing, degradation of wood cell walls, as well as changes in EMC. The specimens were occasionally underwater during the rainy season and after snow melting. Therefore, fungal spore infection, partial disintegration and delamination may occur in cell walls of wood after a long-term soaking and weathering (Xing et al. 2015), resulting in a decrease in hardness. In addition, the increase in EMC decreases the resistance to load, which may be another reason for the decreasing hardness (see Chapter 3.1.4. Kulasinski et al. 2015; Peng et al. 2016).

Table 6. The average basic density of specimens during weathering (kg/m^3 , C: control, S: Thermo S, D: Thermo D, I: copper salt impregnated)

Species	Scots pine				Norway spruce			European ash		
	C	I	S	D	C	S	D	C	S	D
Mean	377.2	386.4	381.3	372.6	368.0	367.0	366.9	550.2	562.3	552.8
Std.	24.5	30.7	26.8	29.2	34.9	27.7	32.0	27.8	33.0	60.7

* The number of specimens in each group is ca. 24 (see Table 3).

Table 7. Brinell hardness of wood as a function of time of natural weathering (MPa, values in parentheses represent standard deviation, C: control, S: Thermo S, D: Thermo D, I: copper salt impregnated)

Period (month)	Scots pine				Norway spruce			European ash		
	C	S	D	I	C	S	D	C	S	D
0	12.7 ^{aA} (2.1)	12.9 ^{aA} (1.6)	12.5 ^{aA} (2.5)	12.7 ^{aA} (2.3)	12.9 ^{aA} (2.2)	11.3 ^{aA} (1.8)	11.3 ^{aA} (2.1)	35.1 ^{bA} (3.9)	33.2 ^{bA} (6.4)	26.3 ^{cA} (6.1)
7	12.1 ^{aA} (2.7)	10.5 ^{aB} (1.7)	10.0 ^{aB} (1.7)	12.4 ^{aA} (2.7)	12.8 ^{aA} (2.2)	10.8 ^{aA} (2.0)	10.7 ^{aA} (1.7)	29.3 ^{cB} (3.3)	26.6 ^{bcB} (5.0)	25.2 ^{bA} (6.6)
12	10.8 ^{aB} (1.9)	10.2 ^{aB} (1.7)	9.9 ^{aB} (2.0)	12.0 ^{aA} (2.5)	11.9 ^{aB} (2.3)	10.1 ^{aB} (2.0)	10.0 ^{aB} (1.6)	26.0 ^{bC} (2.8)	25.1 ^{bBC} (4.4)	23.2 ^{bB} (6.0)
19	10.6 ^{aB} (1.7)	10.3 ^{aB} (1.5)	9.3 ^{aC} (1.9)	10.9 ^{aB} (2.1)	11.9 ^{aB} (2.1)	9.7 ^{aB} (1.6)	9.5 ^{aB} (1.6)	24.1 ^{bD} (2.2)	24.9 ^{bC} (4.1)	21.0 ^{cC} (5.3)
24	9.0 ^{aC} (1.3)	9.1 ^{aC} (1.7)	8.8 ^{aC} (1.6)	10.3 ^{aC} (2.0)	10.1 ^{aC} (2.9)	8.7 ^{aC} (1.5)	8.2 ^{aC} (1.3)	20.1 ^{bE} (2.3)	21.2 ^{bD} (3.4)	20.3 ^{bD} (5.3)

* Different capital letters (A–E) within each column indicate significant difference by Paired Samples Test ($P < 0.05$). Different small letters (a-e) in each row indicate significant difference by One-way ANOVA Test ($P < 0.05$).

3.3 Reliability and validity of the results

The objective of this thesis was to investigate the effects of water and weather exposure on the chemical properties, cellular structure, and physical properties of thermally modified Scots pine, Norway spruce and European ash. The most widespread thermal modification, the ThermoWood® process, was used as the modification method. Two modification classes, Thermo S and Thermo D, were compared. To achieve the study objectives, the experiments were carried out using three different exposure conditions: humid, long-term water contact, and irregular water contact outdoor exposure conditions.

Surface chemistry and pH were analyzed to evaluate the effect of water and weather exposure on chemical changes. The effect of different exposures on cellular structure was observed and measured by microscopy and NMR cryoporometry. Physical properties such as basic density, EMC, FSP, swelling and shrinkage, color, cracking, cupping and hardness were also studied at different exposure conditions. Each experiment was repeatedly measured from the same specimen or a specimen prepared from the successive section of the same board. Several measurement positions and average values were used to eliminate the variation of different materials as much as possible.

More detailed analyses are needed to further understand all the changes taking place in TMW under their real service conditions. These include:

- 1) increasing the number of replicates for some measurements. For most of the measurements, the number of replicates is considered sufficient, and the results obtained are considered reasonable and reliable. However, the number of replicates for pH and FTIR measurements in the LWC test, as well as NMR and cracking measurements in the NW test was small, and could be improved to increase the reliability of the results.

2) adding a reference group of coated (oils, waxes, varnish) TMW to the NW test would be helpful to predict the TMW products in practical service conditions, because surface treatment is usually applied in reality to protect TMW from moisture and UV radiation-induced changes.

3) adding analysis of the soaking liquid in the LWC test would aid in better understanding of the wood constitution degradation products, and hyphae identification to predict the fungal attack in similar conditions.

4) increasing wetting-drying cycles in the T-RH test. In the present study, three T-RH conditions were studied individually. Increasing the wetting-drying cycles would be helpful to understand the effect of absorption/desorption hysteresis on TMW.

5) extending the NW test period up to several decades. Although the results show that the degradation of wood takes place already within two years, a two-year NW period represents just the initial phase of a wood product's service life. Extending the test period would be beneficial to evaluate the performance of TMW products during their entire service life.

6) adding strength analysis of TMW (i.e. modulus of rupture, modulus of elasticity, impact bending) after long-term weathering/water soaking to provide useful strength information of TMW applications.

7) adding an additional experiment examining the cyclic freezing-thawing of wet TMW under controlled conditions would be beneficial to simulate the cold winter and especially mimicking the autumn and spring conditions of temperature fluctuations in the Nordic region.

8) analysis of cupping, warping, or twisting behavior of boards with well-described annual ring orientation and growth rate information.

9) adding study of creep and relaxation behavior of TMW to understand the performance of TMW under load.

4 CONCLUSIONS

Scots pine (*Pinus sylvestris*), Norway spruce (*Picea abies*), and European ash (*Fraxinus excelsior*) boards were thermally modified into two classes, Thermo S and Thermo D, by the industrial ThermoWood® process. The effects of moisture, liquid water and wet natural environment on the chemical composition, microstructure, and physical properties of TMW were then determined. Unmodified wood and copper salt-impregnated pine boards were used as controls. The performance of both modified and control wood under different exposure conditions were evaluated.

In different temperature-relative humidity (T-RH) and long-term water contact (LWC) exposure, TMW absorbs less water from the surrounding air and shows lower EMC and better dimensional stability than unmodified wood in different T-RH conditions. An increase in TM intensity reduces the EMC and improves the dimensional stability of wood mostly in the tangential direction. Brinell hardness decreases with increasing EMC, and the TMW showed lower hardness compared with that of unmodified wood only in the most humid environment tested (10 °C and 90% RH). The FTIR analysis showed that hemicelluloses and cellulose are more prone to changes in long-term water exposure than lignin. Even though TM generally increases the relative crystallinity of cellulose via degradation of its amorphous domains and decreases wood hygroscopicity, long-term water contact increases wood hygroscopicity again. In addition, the initial lower pH level of TMW tends to promote the degradation of the cell-wall compounds, resulting in faster degradation of the TMW compared to unmodified

wood. Impregnation with copper salt does not have an important contribution to the EMC, dimensional stability, or Brinell hardness of Scots pine.

In natural weathering (NW) exposure, clear degradation of lignin on wood surface happened in the first seven months of weathering and leaching of the degradation products leaves a grey hue wood surface rich in cellulose and hemicellulose. TMW presented fewer changes in lignin structure and color due to its lower hygroscopicity and condensed lignin structure compared to unmodified wood. Weathering also degrades cell wall and increases the FSP, indicating increase in water accessibility, more clearly in TMW than in unmodified wood. TMW has less cell wall pores than unmodified wood, and weathering increases the number of pores mainly by increasing the number of available bound water sites rather than of interfibrillar voids. The EMC of all treatment groups increased as a function of weathering time. Although TMW has lower EMC during weathering, the increase rate was higher for TMW than for unmodified wood. Brinell hardness decreased gradually due to the cell wall degradation and increase in EMC. New checks were more frequently observed in TMW than in unmodified wood and more frequently in Scots pine than in Norway spruce and European ash wood. Although TM cannot prevent cupping, TMW showed less cupping compared to unmodified wood in the wet conditions. These findings also confirm that by increase in TM intensity, TMW obtains characteristic reduced surface chemical changes, water accessibility, and cell wall pores that improve its weathering performance compared to unmodified wood. Copper salt impregnation also shows less changes in lignin structure and better color stability than unmodified wood, which is because the reaction of copper salt with phenolic groups of lignin retards the formation of new chromophores. In addition, impregnated samples showed the same tendency of changes in EMC and hardness as unmodified wood, and less cracking compared to TMW after weathering.

In conclusion, TMW, which has lower hygroscopicity, higher dimensional stability, more checks and relatively more damaged microstructure compared to unmodified wood, are well-suited to non-structural applications involving high humidity or frequent water contact conditions. Moreover, Thermo D modification can be used in more demanding environmental conditions than Thermo S. Copper salt impregnation does not improve the water resistance of wood, but it improves the color stability against photodegradation. On top of this, further detailed analyses are needed to provide a more realistic picture of the underlying processes of TMW during usage (see: Chapter 3.3).

5 REFERENCES

Ahmed SA., Hansson L., Morén T. (2013). Distribution of preservatives in thermally modified Scots pine and Norway spruce sapwood. *Wood Science and Technology* 47: 499-513. <https://doi.org/10.1007/s00226-012-0509-4>

Ahmed SA., Morén T. (2012). Moisture properties of heat-treated Scots pine and Norway spruce sapwood impregnated with wood preservatives. *Wood and Fiber Science* 44(1): 85-93

Almeida G., Gagné S., Hernández R. (2007). A NMR study of water distribution in hardwoods at several equilibrium moisture contents. *Wood Science and Technology* 41(4): 293-307. <https://doi.org/10.1007/s00226-006-0116-3>

Altgen M., Hofmann T., Militz H. (2016). Wood moisture content during the thermal modification process affects the improvement in hygroscopicity of Scots pine sapwood. *Wood Science and Technology* 50(6): 1181-1195. <https://doi.org/10.1007/s00226-016-0845-x>

Altgen M., Militz H. (2015). Effect of temperature and steam pressure during the thermal modification process. 8th European Conference on Wood Modification, Helsinki, Finland 226-233.

Akgül M., Gumuskaya E., Korkut S. (2007). Crystalline structure of heat-treated Scots pine (*Pinus sylvestris* L.) and Uludag fir (*Abies nordmannia* (Stev.) subsp. *bornmuelleriana*) wood. *Wood Science and Technology* 41(3): 281-289. <https://doi.org/10.1007/s00226-006-0110-9>

Aksnes DW., Førlund K., Kimtys L. (2001). Pore size distribution in mesoporous materials as studied by ¹H NMR. *Physical Chemistry Chemical Physics* 3(15): 3203-3207. <https://doi.org/10.1039/b103228n>

Aksnes DW., Kimtys L. (2004). ¹H and ²H NMR studies of benzene confined in porous solids: Melting point depression and pore size distribution. *Solid State Nuclear Magnetic Resonance* 25: 146-152. <https://doi.org/10.1016/j.ssnmr.2003.03.001>

Alén R., Kotilainen R., Zaman A. (2002). Thermochemical behavior of Norway spruce (*Picea abies*) at 180-225 °C. *Wood Science and Technology* 36: 163-171. <https://doi.org/10.1007/s00226-001-0133-1>

Andersson S., Serimaa R., Väänänen T., Paakkari T., Jämsä S., Viitaniemi P. (2005). X-ray scattering studies of thermally modified Scots pine (*Pinus sylvestris* L.). *Holzforschung* 59: 422-427. <https://doi.org/10.1515/HF.2005.069>

Avni E., Davoudzadeh F., Coughlin RW. (1985). Flash pyrolysis of lignin. In: Overend R.P., Milne. T.A., Mudge. L.K. (eds.). *Fundamental of thermochemical biomass conversion*. London, Great Britain, 329-343. https://doi.org/10.1007/978-94-009-4932-4_18

Awoyemi L., Jones IP. (2011). Anatomical explanations for the changes in the properties of western red cedar (*Thuja plicata*) wood during heat treatment. *Wood Science and Technology* 45: 261-267. <https://doi.org/10.1007/s00226-010-0315-9>

Ayadi N., Lejeune F., Charrier F., Charrier B., Merlin A. (2003). Color stability of heat treated wood during artificial weathering. *Holz als Roh-und Werkstoff* 61: 221-226. <https://doi.org/10.1007/s00107-003-0389-2>

Bhuiyan TR., Hirai N., Sobue N. (2000). Changes of crystallinity in wood cellulose by heat treatment under dried and moist conditions. *Journal of Wood Science* 46(6): 431-436. <https://doi.org/10.1007/BF00765800>

Bhuiyan TR., Hirai N. (2005). Study of crystalline behavior of heat-treated wood cellulose during treatments in water. *Journal of Wood Science* 51(1): 42-47. <https://doi.org/10.1007/s10086-003-0615-x>

Booker RE., Evans JM. (1994). The effect of drying schedule on the radial permeability of *Pinus radiata* D. Don. *European Journal of Wood and Wood Products* 52: 150-156. <https://doi.org/10.1007/BF02615211>

Boonstra MJ., Acker J., Tjeerdsma B., Kegel E. (2007). Strength properties of thermally modified softwoods and its relation to polymeric structural wood constituents. *Annals of Forest Science* 64(7): 679-690. <https://doi.org/10.1051/forest:2007048>

Boonstra MJ., Rijdsdijk JF., Sander C., Kegel E., Tjeerdsma B., Militz H., Van Acker J., Stevens M. (2006a). Microstructural and physical aspects of heat treated wood. Part 1. Softwoods. *Maderas-Ciencia y Tecnología* 8: 193-208. <https://doi.org/10.4067/S0718-221X2006000300007>

Boonstra MJ., Rijdsdijk JF., Sander C., Kegel E., Tjeerdsma B., Militz H., Van Acker J., Stevens M. (2006b). Microstructural and physical aspects of heat treated wood. Part 2. Hardwoods. *Maderas-Ciencia y Tecnología* 8: 209-217. <https://doi.org/10.4067/S0718-221X2006000300007>

Boonstra MJ., Tjeerdsma B. (2006). Chemical analysis of heat treated softwoods. *Holz als Roh-und Werkstoff* 64: 204-211. <https://doi.org/10.1007/s00107-005-0078-4>

Borrega M., Kärenlampi PP. (2008). Effect of relative humidity on thermal degradation of Norway spruce (*Picea abies*) wood. *Journal of Wood Science* 54: 323-328. <https://doi.org/10.1007/s10086-008-0953-9>

Borrega M., Nevalainen S., Heräjärvi H. (2009). Resistance of European and hybrid aspen wood against two brown-rot fungi. *European Journal of Wood and Wood Products* 67: 177-182. <https://doi.org/10.1007/s00107-009-0322-4>

Chen CM., Wangaard F. (1968). Wettability and the hysteresis effect in the sorption of water vapor by wood. *Wood Science and Technology* 2(3): 177-187

Colom X., Carrillo F., Nogués F., Garriga P. (2003). Structural analysis of photodegraded wood by means of FTIR spectroscopy. *Polymer Degradation and Stability* 80: 543-549. [https://doi.org/10.1016/S0141-3910\(03\)00051-X](https://doi.org/10.1016/S0141-3910(03)00051-X)

Deka M., Humar M., Rep G., Kričej B., Šentjurc M., Petrič M. (2008). Effects of UV light irradiation on color stability of thermally modified, copper ethanolamine treated and non-modified wood: EPR and DRIFT spectroscopic studies. *Wood Science and Technology* 42(1): 5-20. <https://doi.org/10.1007/s00226-007-0147-4>

Eaton RA., Hale MDC. (1993). *Wood: Decay Pests and Protection*, Chapman & Hall, London

Esteves B., Domingos I., Pereira H. (2007b). Improvement of technological quality of eucalypt wood by heat treatment in air at 170-200°C. *Forest Products Journal* 57(1): 47-52

Esteves B., Domingos I., Pereira H. (2008a). Pine wood modification by heat treatment in air. *BioResources* 3(1): 142-154.

Esteves B., Graca J., Pereira H. (2008b). Extractive composition and summative chemical analysis of thermally treated eucalypt wood. *Holzforschung* 62: 344-351. <https://doi.org/10.1515/HF.2008.057>

Esteves B., Pereira H. (2009). Wood modification by heat treatment: a review. *BioResources* 4(1): 370-404.

Esteves B., Velez Marques A., Domingos I., Pereira H. (2008c). Heat-induced color changes of pine (*Pinus pinaster*) and eucalypt (*Eucalyptus globulus*) Wood. *Wood Science and Technology* 42(5): 369-384. <https://doi.org/10.1007/s00226-007-0157-2>

Esteves B., Velez Marques A., Domingos I., Pereira H. (2007). Influence of steam heating on the properties of pine (*Pinus pinaster*) and eucalypt (*Eucalyptus globulus*) wood. *Wood Science and Technology* 41: 193-207. <https://doi.org/10.1007/s00226-006-0099-0>

Evans PD., Thay PD., Schmalzl KJ. (1996). Degradation of wood surfaces during natural weathering. Effects on lignin and cellulose and on the adhesion of acrylic latex primers. *Wood Science and Technology* 30: 411-422. <https://doi.org/10.1007/BF00244437>

Feist WC., Sell J. (1987). Weathering behavior of dimensionally stabilized wood treated by heating under pressure of nitrogen gas. *Wood and Fiber Science* 19(2): 183-195

Fengel D., Wegener G. (1989). *Wood: Chemistry, Ultrastructure, Reaction*. Walter de Gruyter, Berlin, Germany

Fredriksson M., Thybring EE. (2019). On sorption hysteresis in wood: Separating hysteresis in cell wall water and capillary water in the full moisture range. *PLoS ONE*. 14(11): e0225111. <https://doi.org/10.1371/journal.pone.0225111>

Fredriksson M., Thygesen LG. (2017). The states of water in Norway spruce (*Picea abies* (L.) Karst.) studied by low-field nuclear magnetic resonance (LFNMR) relaxometry: assignment of free-water populations based on quantitative wood anatomy. *Holzforschung* 71(1): 77-90. <https://doi.org/10.1515/hf-2016-0044>

Gao X., Zhuang S., Jin J., Cao P. (2015). Bound Water Content and Pore Size Distribution in Swollen Cell Walls Determined by NMR Technology. *BioResources* 10(4): 8208-8224. <https://doi.org/10.15376/biores.10.4.8208-8224>

Gezici-Koç Ö., Erich S., Huinink H., Ven L., Adan O. (2017). Bound and free water distribution in wood during water uptake and drying as measured by 1D magnetic resonance imaging. *Cellulose* 24(2): 535-553. <https://doi.org/10.1007/s10570-016-1173-x>

Glass SV., Zelinka SL. (2010). *Moisture Relations and Physical Properties of Wood*. Wood handbook: wood as an engineering material: chapter 4. Centennial ed. General technical report FPL-GTR-190. Madison, WI: U.S. Dept. of Agriculture, Forest Service, Forest Products Laboratory, p. 4.1-4.19.

Glasser W. (2019). About Making Lignin Great Again-Some Lessons From the Past. *Frontiers in Chemistry* 7: 1-17. <https://doi.org/10.3389/fchem.2019.00565>

Gonzalez-Peña MM., Curling SF., Hale MDC. (2009). On the effect of heat on the chemical composition and dimensions of thermally modified wood. *Polymer Degradation and Stability* 94: 2184-2193. <https://doi.org/10.1016/j.polymdegradstab.2009.09.003>

Gosselink R., Krosse A., Van der Putten J., Van der Kolk J., de Klerk-Engels B., van Dam J. (2004). Wood preservation by low-temperature carbonization. *Industrial Crops and Products* 19: 3-12. [https://doi.org/10.1016/S0926-6690\(03\)00037-2](https://doi.org/10.1016/S0926-6690(03)00037-2)

Hansen EW., Stöcker M., Schmidt R. (1996). Low-Temperature Phase Transition of Water Confined in Mesopores Probed by NMR. Influence on Pore Size Distribution. *The Journal of Physical Chemistry* 100(6): 2195-2200. <https://doi.org/10.1021/jp951772y>

Heräjärvi H. (2009). Effect of drying technology on aspen wood properties. *Silva Fennica* 43(3): 433-445. <https://doi.org/10.14214/sf.198>

Herrera R., Erdocia X., Llano-Ponte R., Labidi J. (2014). Characterization of hydrothermally treated wood in relation to changes on its chemical composition and physical properties. *Journal of Analytical and Applied Pyrolysis* 107: 256-266. <https://doi.org/10.1016/j.jaap.2014.03.010>

Herrera-Díaz R., Sepúlveda-Villaruel V., Pérez-Peña N., Salvo-Sepúlveda L., Salinas-Lira C., Llano-Ponte R., Ananías RA. (2018). Effect of wood drying and heat modification on some physical and mechanical properties of radiata pine. *Drying Technology* 36(5): 537-544. <https://doi.org/10.1080/07373937.2017.1342094>

Hietala S., Maunu SL., Sundholm F., Jämsä S., Viitaniemi P. (2002). Structure of Thermally Modified Wood Studied by Liquid State NMR Measurements. *Holzforschung* 56: 522-528. <https://doi.org/10.1515/HF.2002.080>

Hill CAS. (2006). *Wood modification - chemical, thermal and other processes*. Chichester, John Wiley & Sons, UK.. <https://doi.org/10.1002/0470021748>

Hoebler C., Barry JL., David A., Delort-Laval J. (1989). Rapid acid hydrolysis of plant cell wall polysaccharides and simplified quantitative determination of their neutral monosaccharides by Gas-Liquid Chromatography. *Journal of Agricultural and Food Chemistry* 37: 360-367. <https://doi.org/10.1021/jf00086a020>

Hon DNS., Ifju G. (1978). Measuring penetration of light into wood by detection of photo-induced free radicals, *Wood Science* 11: 118-127.

Hon DNS., Feist WC. (1992). Hydroperoxidation in photoirradiated wood surface. *Wood and Fiber Science* 24: 448-455.

Hon D., Shiraishi N. (2001). *Wood and cellulosic chemistry*. Marcel Dekker, Inc, New York, USA. <https://doi.org/10.1201/9781482269741>

Huang X., Kocafe D., Kocafe Y., Boluk Y., Krause C. (2013). Structural analysis of heat-treated birch (*Betula papyrifera*) surface during artificial weathering. *Applied Surface Science* 264: 117-127. <https://doi.org/10.1016/j.apsusc.2012.09.137>

Huang X., Kocafe D., Kocafe Y., Boluk Y., Pichette A. (2012). A spectrophotometric and chemical study on color modification of heat-treated wood during artificial weathering. *Applied Surface Science* 258: 5360-5369. <https://doi.org/10.1016/j.apsusc.2012.02.005>

Huang X., Kocafe D., Kocafe Y., Boluk Y., Pichette A. (2012b). Changes in wettability of heat-treated wood due to artificial weathering. *Wood Science and Technology* 46(6): 1215-1237. <https://doi.org/10.1007/s00226-012-0479-6>

Huang X., Kocafe D., Kocafe Y., Boluk Y., Pichette A. (2012c). Study of the degradation behavior of heat-treated jack pine (*Pinus banksiana*) under artificial sunlight irradiation. *Polymer Degradation and Stability* 97(7): 1197-1214. <https://doi.org/10.1016/j.polymdegradstab.2012.03.022>

Jackson CL., McKenna GB. (1990). The melting behavior of organic materials confined in porous solids. *The Journal of Chemical Physics* 93(12): 9002-9011. <https://doi.org/10.1063/1.459240>

Jämsä S., Ahola P., Viitaniemi P. (2000). Long-term natural weathering of coated ThermoWood. *Pigment and Resin Technology* 29(2): 68-74. <https://doi.org/10.1108/03699420010317807>

Javed MA., Kekkonen PM., Ahola S., Telkki V-V. (2015). Magnetic resonance imaging study of water absorption in thermally modified pine wood. *Holzforschung* 69(7): 899-907. <https://doi.org/10.1515/hf-2014-0183>

Kacík F., Smíra P., Kacíková D., Vel'ková V., Nasswetrová A., Vacek V. (2015). Chemical alterations of pine wood saccharides during heat sterilization. *Carbohydrate Polymers* 117: 681-686. <https://doi.org/10.1016/j.carbpol.2014.10.065>

Kalnins M., Feist W. (1993). Increase in wettability of wood with weathering. *Forest Products Journal* 43(2): 55

Kamdem D., Pizzi A., Jermannaud A. (2002). Durability of heat-treated wood. *Holz als Roh-und Werkstoff* 60: 1-6. <https://doi.org/10.1007/s00107-001-0261-1>

Kekkonen PM., Ylisassi A., Telkki V-V. (2014). Absorption of Water in Thermally Modified Pine Wood As Studied by Nuclear Magnetic Resonance. *The Journal of Physical Chemistry C* 118(4): 2146-2153. <https://doi.org/10.1021/jp411199r>

Kettunen PO. (2006). *Wood structure and properties*. Trans Tech Publications Ltd, Uetikon-Zuerich, Switzerland

Kocafe D., Poncsák S., Boluk Y. (2008). Effect of thermal treatment on the chemical composition and mechanical properties of birch and aspen. *BioResources* 3(2): 517-537

Kollmann F., Côté WA. (1968). Principles of wood science and technology. 1. Solid wood. Springer-Verlag. Berlin, Heidelberg, New York.. <https://doi.org/10.1007/978-3-642-87928-9>

Korkut S., Akgul M., Dundar T. (2008a). The effects of heat treatment on some technological properties of Scots pine wood. *Bioresource Technology* 99: 1861-1868. <https://doi.org/10.1016/j.biortech.2007.03.038>

Korkut S., Kök MS., Korkut DS., Gürleyen T. (2008b). The effects of heat treatment on technological properties in Red-bud maple (*Acer trautvetteri* Medw.) wood. *Bioresource Technology* 99(6): 1538-1543. <https://doi.org/10.1016/j.biortech.2007.04.021>

Książczak A., Radomski A., Zielenkiewicz T. (2003). Nitrocellulose porosity - thermopometry. *Journal of Thermal Analysis and Calorimetry* 74(2): 559-568. <https://doi.org/10.1023/B:JTAN.0000005194.70360.c1>

Kulasinski K., Guyer R., Keten S., Derome D., Carmeliet J. (2015). Impact of moisture adsorption on structure and physical properties of amorphous biopolymers. *Macromolecules* 48: 2793-2800. <https://doi.org/10.1021/acs.macromol.5b00248>

Labbé N., De Jéso B., Lartigue JC., Daudé G., Pétraud M., Ratier M. (2002). Moisture Content and Extractive Materials in Maritime Pine Wood by Low Field 1H NMR. *Holzforschung* 56(1): 25-31. <https://doi.org/10.1515/HF.2002.005>

Labbé N., De Jéso B., Lartigue J., Daudé G., Pétraud M., Ratier M. (2006). Time-domain 1 H NMR characterization of the liquid phase in greenwood. *Holzforschung* 60(3): 265-270. <https://doi.org/10.1515/HF.2006.043>

Metsä-Kortelainen S., Antikainen T., Viitaniemi P. (2006). The water absorption of sapwood and heartwood of Scots pine and Norway spruce heat-treated at 170°C, 190°C, 210°C and 230°C. *Holz als Roh-und Werkstoff* 64(3): 192-197. <https://doi.org/10.1007/s00107-005-0063-y>

Mitchell J., Webber JBW., Strange JH. (2008). Nuclear Magnetic Resonance Cryoporometry. *Physics Reports* 461: 1-36. <https://doi.org/10.1016/j.physrep.2008.02.001>

Mitchell PH. (1988). Irreversible property changes of small loblolly pine specimens heated in air, nitrogen, or oxygen. *Wood and Fiber Science* 3: 320-335

Monties B. (2003). Botanical variability and mechanical function of lignins, two critical aspects of the plant phenolic secondary metabolism. *Advances Phytochemistry* 1-48.

Nuopponen M., Vuorinen T., Jämsä S., Viitaniemi P. (2003). The effects of a heat treatment on the behavior of extractives in softwood studied by FTIR spectroscopic methods. *Wood Science and Technology* 37: 109-115. <https://doi.org/10.1007/s00226-003-0178-4>

Nuopponen M., Wikberg H., Vuorinen T., Maunu SL., Jämsä S., Viitaniemi P. (2004). Heat-treated softwood exposed to weathering. *Journal of Applied Polymer Science* 91: 2128-2134. <https://doi.org/10.1002/app.13351>

Peng H., Jiang J., Zhan T., Lu J. (2016). Influence of density and equilibrium moisture content on the hardness anisotropy of wood. *Forest Products Journal* 66: 443-452. <https://doi.org/10.13073/FPJ-D-15-00072>

Petrov O., Furo I. (2006). Curvature-Dependent Metastability of the Solid Phase and the Freezing-Melting Hysteresis in Pores. *Physical Review E* 73: No. 011608. <https://doi.org/10.1103/PhysRevE.73.011608>

Poncsák S., Kocaefe D., Bouazara M., Pichette A. (2006). Effect of high temperature treatment on the mechanical properties of birch (*Betula papyrifera*). *Wood Science and Technology* 40(8): 647-663. <https://doi.org/10.1007/s00226-006-0082-9>

Priadi T., Hiziroglu S. (2013). Characterization of heat treated wood species. *Materials and Design* 49: 575-582. <https://doi.org/10.1016/j.matdes.2012.12.067>

- Rapp AO. (2001). European thematic network for wood modification - review on heat treatments of wood. BFH, Hamburg, Germany
- Rowell RM. (2012). Handbook of wood chemistry and wood composites. Taylor & Francis Group, Boca Raton, USA. <https://doi.org/10.1201/b12487>
- Salmén L. (2004). Micromechanical understanding of the cell-wall structure. *Comptes rendus - Biologies* 327(9): 873-880. <https://doi.org/10.1016/j.crvi.2004.03.010>
- Sandberg D. (1999). Weathering of radial and tangential wood surfaces of pine and spruce. *Holzforschung* 53(4): 355-364. <https://doi.org/10.1515/HF.1999.059>
- Sandberg D., Kutnar A., Mantanis G. (2017). Wood modification technologies - a review. *iForest- Biogeosciences and Forestry* 10(6): 895-908. <https://doi.org/10.3832/ifer2380-010>
- Siau JF. (1995). Wood: influence of moisture on physical properties. Dept. of Wood Science and Forest Products, Virginia Polytechnic Institute and State University, VA
- Sjöström E. (1993). Wood chemistry: Fundamentals and applications. Academic Press. San Diego, CA. USA
- Skaar C. (1988). Wood-Water Relations. In: Springer series in wood science. Springer-Verlag. Berlin. Heidelberg.. <https://doi.org/10.1007/978-3-642-73683-4>
- Srinivas K., Pandey KK. (2012). Photodegradation of thermally modified wood. *Journal of Photochemistry and Photobiology* 117: 140-145. <https://doi.org/10.1016/j.jphoto-biol.2012.09.013>
- Stamm AJ. (1956). Thermal degradation of wood and cellulose. *Journal of Industrial and Engineering Chemistry* 48: 413-417. <https://doi.org/10.1021/ie51398a022>
- Sundqvist B. (2004). Color changes and acid formation in wood during heating. Ph.D. thesis in Division of Wood Material Science. Lulea University of technology, Sweden
- Telkki V-V. (2018). Hyperpolarized Laplace NMR. *Magnetic Resonance in Chemistry* 56(7): 619-632. <https://doi.org/10.1002/mrc.4722>
- Telkki V-V., Yliniemi M., Jokisaari J. (2013). Moisture in softwoods: fiber saturation point, hydroxyl site content, and the amount of micropores as determined from NMR relaxation time distributions. *Holzforschung* 67(3): 291-300. <https://doi.org/10.1515/hf-2012-0057>
- Temiz A., Terziev N., Eikenes M., Hafren J. (2007). Effect of accelerated weathering on surface chemistry of modified wood. *Applied Surface Science* 253: 5355-5362. <https://doi.org/10.1016/j.apsusc.2006.12.005>
- Temiz A., Terziev N., Jacobsen B., Eikenes M. (2006). Weathering, water absorption, and durability of silicon, acetylated, and heat-treated wood. *Journal of Applied Polymer Science* 102: 4506-4513. <https://doi.org/10.1002/app.24878>
- ThermoWood Handbook. (2003). International ThermoWood Association, URI: https://asiakas.kotisivukone.com/files/en.thermowood.palvelee.fi/downloads/tw_handbook_080813.pdf. Cited 29.9.2019.
- ThermoWood Production Statistics. (2018). International ThermoWood Association, URI: <https://asiakas.kotisivukone.com/files/en.thermowood.palvelee.fi/uutiset/Production-statistics2018.pdf>. Cited 29.9.2019
- Thomas RJ. (1977). Wood: structure and chemical composition. In *Wood Technology: Chemical Aspects*; Goldstein, I. ACS Symposium Series; American Chemical Society, Washington, DC, pp.1-23. <https://doi.org/10.1021/bk-1977-0043.ch001>
- Thybring EE., Kymäläinen M., Rautkari L. (2018). Experimental techniques for characterising water in wood covering the range from dry to fully water-saturated. *Wood Science and Technology* 52: 297-329. <https://doi.org/10.1007/s00226-017-0977-7>
- Tiemann HD. (1906). Effect of moisture upon strength and stiffness of wood. US department of Agriculture Forest Services, Bulletin 70, Washington, DC, 144 pp

Tjeerdsma BF., Boonstra M., Pizzi A., Tekely P., Militz H. (1998). Characterisation of thermally modified wood: molecular reasons for wood performance improvement. *Holz als Roh-und Werkstoff* 56: 149-153. <https://doi.org/10.1007/s001070050287>

Tjeerdsma BF., Militz H. (2005). Chemical changes in hydrothermal treated wood: FTIR analysis of combined hydrothermal and dry heat-treated wood. *Holz als Roh-und Werkstoff* 63: 102-111. <https://doi.org/10.1007/s00107-004-0532-8>

Tolvaj L., Faix O. (1995). Artificial Ageing of Wood Monitored by DRIFT Spectroscopy and CIE L*a*b* Color Measurements. 1. Effect of UV Light. *Holzforschung-Int. J. Biol., Chem., Phys. Technol. Wood.* 49: 397-404. <https://doi.org/10.1515/hfsg.1995.49.5.397>

Tomak ED., Ustaomer D., Ermeydan MA., Yildiz S. (2018). An investigation of surface properties of thermally modified wood during natural weathering for 48 months. *Measurement* 127: 187-197. <https://doi.org/10.1016/j.measurement.2018.05.102>

Tomak ED., Ustaomer D., Yildiz S., Pesman E. (2014). Changes in surface and mechanical properties of heat treated wood during natural weathering. *Measurement* 53: 30-39. <https://doi.org/10.1016/j.measurement.2014.03.018>

Vernois M. (2001). Heat treatment of wood in France-State of the art. In *Review on heat treatments of wood. Proceedings of Special Seminar of Cost Action E22, Antibes, France*

Vincent JF. (1999). From cellulose to cell. *Journal of Experimental Biology* 202: 3263-3268

Weiland JJ., Guyonnet R. (2003). Study of chemical modifications and fungi degradation of thermally modified wood using DRIFT spectroscopy. *Holz als Roh-und Werkstoff* 61: 216-220. <https://doi.org/10.1007/s00107-003-0364-y>

Williams RS. (2005). Weathering of wood, in: R.M. Rowell (Ed.), *Handbook of Wood Chemistry and Wood Composites*, CRC Press, Boca Raton, pp.142-185.

Xing D., Wang S., Li J. (2015). Effect of Artificial Weathering on the Properties of Industrial-Scale Thermally Modified Wood. *BioResources* 10: 8238-8252. <https://doi.org/10.15376/biores.10.4.8238-8252>

Yildiz S., Gezer ED., Yildiz UC. (2006). Mechanical and chemical behavior of spruce wood modified by heat. *Building and Environment* 41: 1762-1766. <https://doi.org/10.1016/j.buildenv.2005.07.017>

Yildiz S., Tomak ED., Yildiz UC., Ustaomer D. (2013). Effect of artificial weathering on the properties of heat treated wood. *Polymer Degradation and Stability* 98(8): 1419-1427. <https://doi.org/10.1016/j.polymdegradstab.2013.05.004>

Yildiz S., Yildiz UC., Tomak ED. (2011). The effects of natural weathering on the properties of heat-treated alder wood. *BioResources* 6: 2504-2521

Zauer M., Kretschmar J., Grossmann L., Pfriem A., Wagenfuhr A. (2014). Analysis of the pore-size distribution and fiber saturation point of native and thermally modified wood using differential scanning calorimetry. *Wood Science and Technology* 48(1): 177-193. <https://doi.org/10.1007/s00226-013-0597-9>